

1 **A Web-based Spatial Decision Support System of Wastewater Surveillance for COVID-19**  
2 **Monitoring: A Case Study of a University Campus**

3

4 Wenwu Tang<sup>a,b\*</sup>, Tianyang Chen<sup>a,b</sup>, Zachery Slocum<sup>a,b</sup>, Yu Lan<sup>a,b</sup>, Eric Delmelle<sup>a,b,c</sup>, Don Chen<sup>d</sup>,  
5 Neha Mittal<sup>e</sup>, Jacelyn Rice-Boayue<sup>d</sup>, Tarini Shukla<sup>b,f</sup>, Sophia Lin<sup>f,g</sup>, Srinivas Akella<sup>h</sup>, Jessica  
6 Schlueter<sup>e</sup>, Mariya Munir<sup>g</sup>, Cynthia Gibas<sup>e</sup>

7

8 <sup>a</sup> Department of Geography and Earth Sciences, University of North Carolina at Charlotte,  
9 Charlotte, NC 28223 USA

10 <sup>b</sup> Center for Applied Geographic Information Science, University of North Carolina at Charlotte,  
11 Charlotte, NC 28223 USA

12 <sup>c</sup> Department of Geographical and Historical Studies, University of Eastern Finland, Joensuu,  
13 Finland

14 <sup>d</sup> Department of Engineering Technology and Construction Management, University of North  
15 Carolina at Charlotte, Charlotte, NC 28223 USA

16 <sup>e</sup> Department of Bioinformatics and Genomics, University of North Carolina at Charlotte,  
17 Charlotte, NC 28223 USA

18 <sup>f</sup> Infrastructure and Environmental System Program, University of North Carolina at Charlotte,  
19 Charlotte, NC 28223 USA

20 <sup>g</sup> Department of Civil & Environmental Engineering, University of North Carolina at Charlotte,  
21 Charlotte, NC 28223 USA

22 <sup>h</sup> Department of Computer Science, University of North Carolina at Charlotte, Charlotte, NC  
23 28223 USA

24 \*Corresponding author, Email: [WenwuTang@uncc.edu](mailto:WenwuTang@uncc.edu), Phone: 1-704-687-5988

25

26 **Abstract**

27 The ongoing COVID-19 pandemic has produced substantial impacts on our society. Wastewater  
28 surveillance has increasingly been introduced to support the monitoring, and thus mitigation, of  
29 COVID-19 outbreaks and transmission. Monitoring of buildings and sub-sewershed areas via a  
30 wastewater surveillance approach has been a cost-effective strategy for mass testing of residents  
31 in congregate living situations such as universities. A series of spatial and spatiotemporal data  
32 are involved with wastewater surveillance, and these data must be interpreted and integrated with  
33 other information to better serve as guidance on response to a positive wastewater signal. The  
34 management and analysis of these data poses a significant challenge, in particular, for the need  
35 of supporting timely decision making. In this study, we present a web-based spatial decision  
36 support system framework to address this challenge. Our study area is the main campus of the  
37 University of North Carolina at Charlotte. We develop a spatiotemporal data model that  
38 facilitates the management of space-time data related to wastewater surveillance. We use  
39 spatiotemporal analysis and modeling to discover spatio-temporal patterns of COVID-19 virus  
40 abundance at wastewater collection sites that may not be readily apparent in wastewater data as  
41 they are routinely collected. Web-based GIS dashboards are implemented to support the  
42 automatic update and sharing of wastewater testing results. Our web-based SDSS framework  
43 enables the efficient and automated management, analytics, and sharing of spatiotemporal data of  
44 wastewater testing results for our study area. This framework provides substantial support for  
45 informing critical decisions or guidelines for the prevention of COVID-19 outbreak and the  
46 mitigation of virus transmission on campus.

47 **Keywords:** Wastewater surveillance, spatial decision support systems, COVID-19, Web GIS

## 48 **1. Introduction**

49 The COVID-19 pandemic has fueled a renewed interest in wastewater-based epidemiology.  
50 Wastewater testing for traces of viral and bacterial pathogens has been used for decades to track  
51 and manage outbreaks of infectious disease (Prado et al., 2012; Tambini et al., 1993). Early  
52 reports in mid-2020 demonstrated that wastewater concentrations of SARS-CoV-2 could serve as  
53 a leading indicator for cases detected by clinical testing within city sewersheds (Ahmed et al.,  
54 2021; Peccia et al., 2020), with collection of samples from wastewater treatment plant influent  
55 providing coverage of entire cities or large neighborhoods. The practical application of  
56 monitoring at city scale is primarily to detect infection trends in communities, which has been  
57 especially useful in the case of COVID-19, both because COVID-19 infections may be  
58 asymptomatic for several days prior to detection of cases by testing, and because especially in  
59 the early months of the pandemic, testing capacity lagged behind the rapid spread of the disease.  
60 In such scenarios, wastewater testing can serve as a leading indicator of the increase of disease  
61 incidence in an urban area. There has also been an increasing interest in monitoring in  
62 neighborhood or smaller scale areas for the presence of the SARS-CoV-2 virus in wastewater,  
63 because such small-scale monitoring can provide evidence to support targeted public health  
64 interventions including distribution of masks or selection of populations for increased testing  
65 (Bowes et al., 2021).

66 COVID-19 is easily transmitted in congregate living situations, with early and devastating  
67 outbreaks being documented in nursing homes and jails (Kırbyık et al., 2020; Lam-Hine et al.,  
68 2021). Beside these, other indoor settings such as schools (including universities), restaurants,  
69 and hospitals have been identified as having high risk for the spread of COVID-19 (Fox et al.,

70 2021; Lam-Hine et al., 2021). Many universities attempted to implement some type of  
71 wastewater surveillance program during the early months of the pandemic, with varying degrees  
72 of success (Gibas et al., 2021; Harris-Lovett et al., 2021; Karthikeyan et al., 2021). To effectively  
73 detect and monitor outbreaks of COVID-19 in these indoor settings requires wastewater  
74 surveillance capabilities at small spatial scales such as building level. The study reported in this  
75 article is focused on building-level wastewater surveillance for COVID-19 monitoring from a  
76 spatiotemporally explicit perspective.

77 Wastewater surveillance typically requires a set of sequential steps, including sample site setup,  
78 sample collection (including storage and shipping; per CDC Wastewater Surveillance strategy),  
79 lab analysis, and subsequent analysis and visualization of wastewater testing results and  
80 associated data. Geographic Information Systems (GIS) methods have been applied for the  
81 management and mapping of spatially explicit data related to wastewater testing and COVID-19  
82 monitoring, and dashboard techniques have gained increasing attention due to their visual  
83 presentation capabilities within web-based environments (Dong et al., 2020; Lan et al., 2021;  
84 Naughton et al., 2021). Yet, most of the existing dashboards for COVID-19 and wastewater  
85 studies only concentrate on management and visualization of relevant spatial or spatiotemporal  
86 data; their support on spatial analytics and modeling capabilities is inadequate. Spatial analytics  
87 and modeling, however, are pivotal in discovering patterns of interest hidden in complicated  
88 spatiotemporal data, and providing predictive or scenario analysis capabilities for monitoring and  
89 mitigation of pandemic situations (Franch-Pardo et al., 2020). Spatial Decision Support Systems  
90 (SDSS) hold potential in filling this gap.

91 SDSS, which originated from the domain of Geographic Information Science (Armstrong et al.,  
92 1986; Sugumaran & Degroote, 2010), have been increasingly applied to assist with decision  
93 making within spatially explicit contexts. SDSS is based on (but more than) the integration of  
94 decision support systems and GIS, and provides inherent support for spatial analytics and  
95 modeling capabilities. This makes SDSS unique and powerful in informing decision making  
96 processes associated with complex spatial or spatiotemporal phenomena. A variety of  
97 applications such as environmental monitoring, natural resources, public health, transportation,  
98 and land use and land cover change have built SDSS to address complex decision problems  
99 within spatially explicit contexts (Delmelle et al., 2014; Keenan & Jankowski, 2019; Sugumaran  
100 & Degroote, 2010). In particular, driven heavily by Internet technologies and cyberinfrastructure  
101 (NSF, 2007), web-based SDSS has received much attention over the past few years (Lan et al.,  
102 2020; Lee et al., 2017; Tayyebi et al., 2016). While a growing body of the literature has  
103 highlighted the power of web-based SDSS, the applications of web-based SDSS for the  
104 resolution of complex spatiotemporal decision problems in general and small-scale wastewater  
105 surveillance for COVID-19 monitoring, in particular, remain scant.

106 In this article, we describe a web-based SDSS framework for building-level wastewater  
107 surveillance. We used a university campus (the main campus of the University of North Carolina  
108 at Charlotte) as a study case. This framework supports the automated synchronization and update  
109 of lab test results, space-time cluster analysis for identifying hotspots of COVID-19 incidents at  
110 the building level over time, and automated update of dashboards within web-based  
111 environments. The integration of these geospatial data and analytics capabilities play a critical  
112 role in providing timely information on COVID-19 incidents in the study region over time.

113 Specifically, we focus on addressing the following sets of research questions in this study: 1) Are  
114 there any space-time clusters of positive wastewater testing results at the building level and  
115 where are they? 2) What are those sampling sites that exhibit similar responses over time in  
116 terms of wastewater testing results and where are they?

117 The remainder of this article is organized using the following structure. In section 2, we discuss  
118 the background and relevant literature of this study. In section 3, we present the study area and  
119 data, the design of the entire web-based SDSS framework as well as its implementation. Section  
120 4 presents the results including space-time cluster analysis, and Section 5 gives relevant  
121 discussion. Section 6 concludes this article.

## 122 **2. Literature Review**

### 123 **2.1. Wastewater Surveillance**

124 A typical workflow for building-level wastewater surveillance includes collection of a sample at  
125 regular intervals with laboratory results within 24 hours of collection. Samples can be collected  
126 using a variety of methods (Medema et al., 2020), ranging from collection of a sample volume at  
127 one timepoint (a “grab” sample), to composites collected by passive sampling for example using  
128 fibrous swabs (Liu et al., 2021), and composites collected using pump autosamplers which add to  
129 the sample at regular intervals over the course of a day prior to collection. Once collected,  
130 samples are processed and concentrated. A wide variety of methods are available for this  
131 concentration step as well, and choice of method is governed by a combination of viral recovery  
132 efficacy, cost, materials availability, and processing time, as described in our previous work  
133 (Juel et al., 2021). RNA is extracted from the concentrated sample, and virus is quantified using

134 a molecular detection protocol such as RT-qPCR or RT-ddPCR (Barua et al., 2021; Ciesielski et  
135 al., 2021), which provides a viral concentration in terms of copies of virus per liter of wastewater  
136 collected. This value can be used effectively as a simple binary indicator of positivity, as  
137 demonstrated in the pilot phase of our campus monitoring program (Gibas et al., 2021) but also  
138 has the potential to connect the information about population size and volume of water used in  
139 the building to provide an estimate of the number of individuals who might be SARS-CoV-2  
140 positive (Sweetapple et al., 2022). Once a positive signal is detected, a decision is made about  
141 whether to test all individuals in that building, after consulting institutional information about  
142 individuals who have recently tested positive or been connected to that site via contact tracing. If  
143 there are no previously-known individuals who are likely to be the source of the positive signal,  
144 then the entire building population is subjected to clinical testing.

145 While many institutions and localities have deployed wastewater testing for SARS-CoV-2 during  
146 the pandemic, only a small fraction of these projects have so far made data available in service of  
147 larger efforts to develop quantitative models and consistent practices in wastewater  
148 epidemiology (Naughton et al., 2021). Data dashboards are a common means for sharing such  
149 information when it is made available, and in some cases have been incorporated into state-level  
150 public health reporting (e.g., see <https://covid19.ncdhhs.gov/dashboard/wastewater-monitoring>).  
151 Dashboard techniques have been extensively applied for the sharing of data related to COVID-  
152 19. A number of dashboards have been developed and deployed to support the wastewater  
153 surveillance initiatives for the monitoring of COVID-19 worldwide. For example, there are a  
154 number of dashboards registered via the web site of COVIDPoops19 project (Naughton et al.,  
155 2021). About 40% of these dashboards have built-in Web GIS functionality. The software

156 platforms used to present these dashboards include Esri ArcGIS Online, Tableau, R Shiny,  
157 Microsoft Power BI, and CARTO. The first three (ArcGIS Online, Tableau, and R Shiny) are the  
158 dominant choices for the implementation of wastewater surveillance dashboards. Most of the  
159 wastewater data managed and reported by these wastewater dashboards are at the wastewater  
160 treatment plant level and collected weekly, while a smaller number of projects report daily or  
161 multiple days per week. A few universities make campus wastewater data available in real time  
162 via public dashboards (e.g. University of California at San Diego, Clemson University), but in  
163 other cases, for instance at the University of North Carolina at Charlotte, the concern of upper  
164 administration not to alarm students or parents with details of wastewater alerts has resulted in a  
165 decision to keep this information for internal use only. A number of existing dashboards only  
166 focus on the visual presentation (in maps or charts) of wastewater-related data, and may not  
167 provide the spatiotemporal analytics and modeling of wastewater testing results and relevant  
168 data. The need for spatiotemporal analysis and modeling to guide the study of wastewater testing  
169 results for the monitoring of COVID-19 outbreak and prevention has been recognized in the  
170 literature (Karthikeyan et al., 2021).

## 171 **2.2. Spatial Decision Support Systems**

172 SDSS are integrative computer-based systems that provide decision-making support for complex  
173 spatial problems via the fusion of spatial data management, modeling, and visualization  
174 capabilities (Densham, 1991; Malczewski, 1999; Sugumaran & Degroote, 2010). SDSS, with an  
175 origin from Decision Support Systems (Marakas, 2003), are distinguished by their ability to  
176 handle decision-making support within a spatially explicit context via the incorporation of GIS-  
177 based functionality. Yet, SDSS differ from GIS in that they encompass spatial modeling



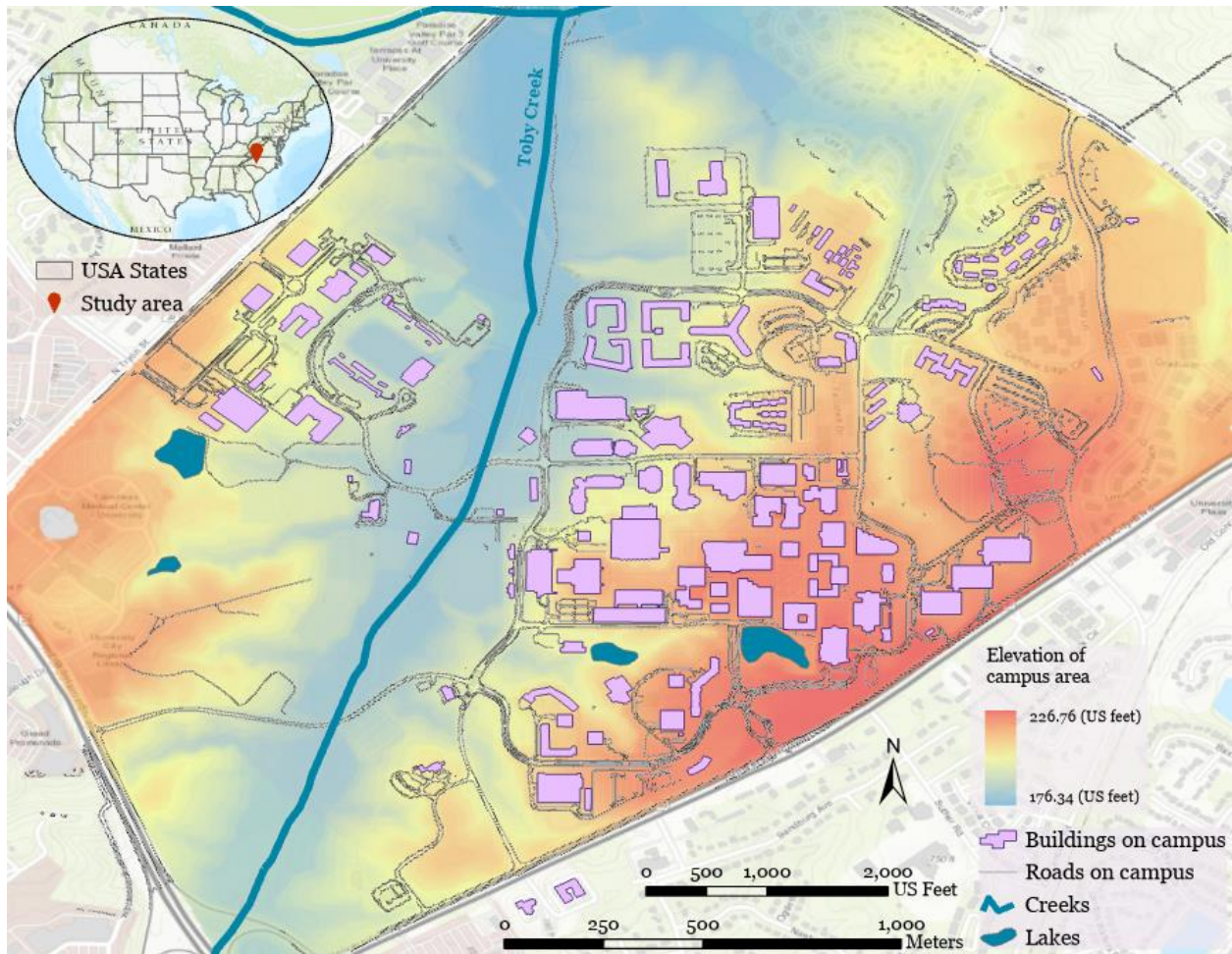
178 capabilities to aid decision-making (Armstrong et al., 1986; Sugumaran & Degroote, 2010). For  
179 example, with the incorporation of a spatial simulation model, SDSS can enable what-if scenario  
180 analysis to explore potential alternative solutions of a spatial problem. The spatial optimization  
181 model helps SDSS identify spatially explicit optimal solutions facing decision makers  
182 (represented by site selection problems). Further, spatial statistical models allow for the  
183 discovery of spatial patterns of interest (e.g., clusters of disease or accidents) from spatial data.  
184 All these modeling capabilities can be built within a SDSS that informs and facilitates decision  
185 making processes associated with complex spatial or spatiotemporal problems (Ghosh, 2008). In  
186 terms of implementation, a SDSS includes the following functional modules: data management,  
187 model management, visualization and report generation, and a user interface (Armstrong et al.,  
188 1986; Densham, 1991; Sugumaran & Degroote, 2010).

189 While the study of SDSS in early stages focuses on the development of conceptual architecture,  
190 cyberinfrastructure-enabled computing technologies such as web and cloud computing have been  
191 fostering the implementation and applications of SDSS into different domain studies (Sugumaran  
192 & Degroote, 2010; Tang et al., 2017). For example, Mwaura and Kada (2017) presented a web-  
193 based SDSS in which a multi-criteria decision making model was used to evaluate potential sites  
194 of geothermal wells in Kenya, east Africa. Crimi et al. (2019) investigated the identification of  
195 priority regions in Bradford, UK for freight lorry parking within a web-based SDSS  
196 environment. Lan et al. (2020) applied web-based SDSS that guides the monitoring and sharing  
197 of water quality information of private wells in Gaston County, NC, USA. Spatial interpolation  
198 algorithms were used in Lan et al.'s work to generate the spatially continuous distribution of  
199 water quality that will inform residents or governments for potential water contamination.

## 200 **3. Materials and Methods**

### 201 **3.1. Study Area and Data**

202 Our study area is the main campus of the University of North Carolina at Charlotte, USA (see  
203 Fig. 1). The main campus of the University (35°18'25"N, 80°44'06"W) is located in the north of  
204 the City of Charlotte (within Mecklenburg County). The University is an urban university with  
205 about 3,000 employees (including faculty and staff); and 30,146 students in the Fall semester of  
206 2020. Among them, around 6,000 students are living in residential halls on campus. In total,  
207 there are 138 buildings in the main campus, 33 residence halls, 32 academic buildings, and 73  
208 other types. Please see Appendix 1 for sources of the aforementioned information about the  
209 University. In terms of topography, the main campus is high in east and west and low in the  
210 middle (range of elevation: 176-226 meters). The slope of the main campus varies from 0° to 25°  
211 (based on a 1-m DEM derived from LiDAR point cloud data). The Toby Creek area is the  
212 lowest-lying region on campus. Toby Creek flows through the campus and discharges into  
213 Mallard Creek at the north end of the campus. The university's sewer system is composed of  
214 gravity sewer lines, where a sampling at a specific sewer manhole location will be affected by  
215 upstream nodes. Lateral and branch sewer lines collect wastewater from all residence and  
216 academic buildings, and then connect to a main sewer line (Charlotte Water's wastewater  
217 system) which parallels Toby Creek. Campus wastewater is treated at the nearby Mallard Creek  
218 Treatment Facility.



219

220 **Fig. 1.** Map of the main campus of the University of North Carolina at Charlotte, USA (sewage  
 221 network details are not shown for the protection of physical security of university infrastructure).

222

223 The University of North Carolina at Charlotte launched its wastewater-based epidemiology  
 224 (WBE) surveillance program in late Summer 2020 to assist the University in monitoring  
 225 COVID-19 incidence. Wastewater signal has been used since that time to identify dormitory  
 226 populations for testing (“surge testing”) in the event of detection of SARS-CoV-2 virus in the  
 227 absence of a previously identified source. The wastewater surveillance program has been  
 228 collecting and analyzing wastewater samples since September, 2020. A team of faculty, staff,

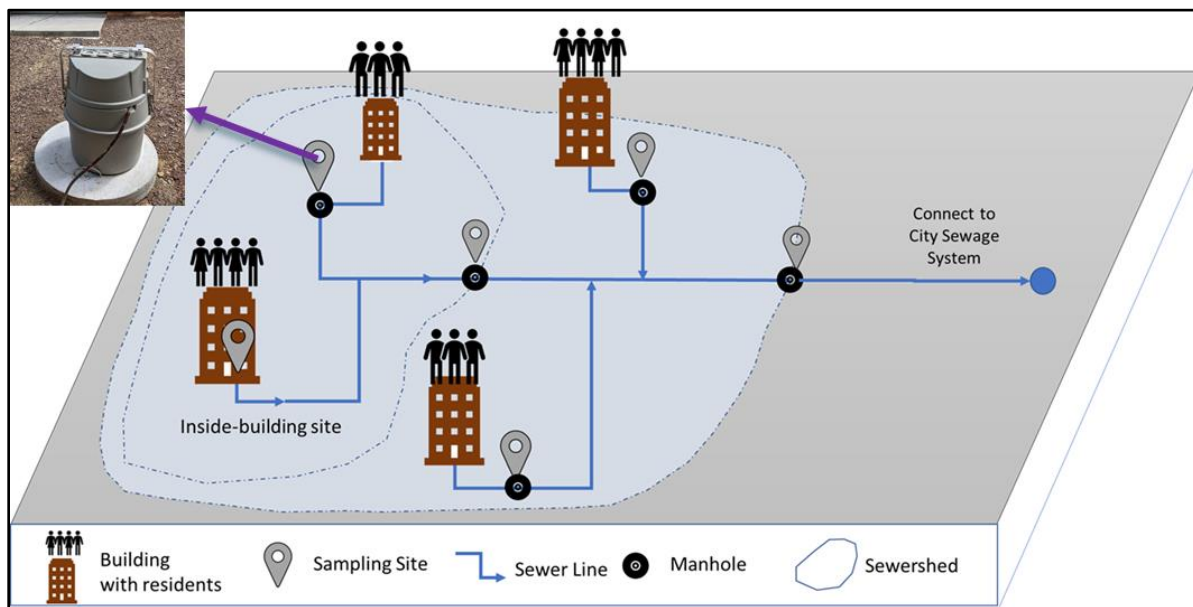
229 and students from bioinformatics, engineering, computer science, and geography collaborate to  
 230 develop this monitoring system, with infrastructure support from the University’s Facilities  
 231 Management staff. The WBE team has also developed a Building Information Modeling (BIM;  
 232 see Becerik-Gerber et al. (2012)) 3D model for each residence hall on campus. Each BIM model  
 233 includes the building envelope and plumbing fixtures, which can be used to identify rooms and  
 234 zones in which potential infected individuals are located. Wastewater data collected together  
 235 with BIM models have allowed campus administration to make timely and targeted decisions to  
 236 prevent the cluster outbreak and spread of COVID-19 on campus (see Gibas et al., 2021 for  
 237 detail). We collected spatial data to support the wastewater surveillance work for our study area.  
 238 These data include buildings, sewer lines, sampling sites, road network, and elevation.

239 Table 1. Spatial data collected for the wastewater surveillance work for the study area.

Spatial Data	Data source	GIS Data Format
Buildings	Department of Facilities Management of UNC Charlotte	Polygon Vector
Sewer lines	Department of Facilities Management of UNC Charlotte	Polyline Vector
Sampling sites	Wastewater Surveillance Task Force Group at UNC Charlotte	Point Vector
Road network	Department of Facilities Management of UNC Charlotte	Polyline Vector
Elevation	U.S. Geological Survey, 3D Elevation Program	Raster

240  
 241 There are in total 38 sampling sites that were identified and established for wastewater collection  
 242 since Fall 2020 (see Fig. 2 for illustration). These sampling sites are organized in two types: for  
 243 residence halls (a sampling site covers a building or part of the building) and for buildings within  
 244 a sub-sewershed—referred to as neighborhood site in this study (a sampling site covers multiple  
 245 buildings). Manholes and plumbing cleanouts are selected to set up these sampling sites. As a  
 246 manhole may connect to multiple sewage lines from different buildings, a manhole may have

247 multiple auto-samplers with probes deployed in different directions (up to two in our study)  
248 installed to collect sewage samples from different buildings. Further, a building (typically large)  
249 may have two or more sampling sites each covering different parts of the building. These  
250 sampling sites cover in total 89 buildings on campus for wastewater monitoring. We used a  
251 Trimble GPS handheld unit (with a submeter accuracy) to obtain the coordinates of the sampling  
252 sites. However, 10 of 38 samplers are located either very close to the building or inside the  
253 building, which degrades the signal quality of GPS satellites. Therefore, their locations are  
254 determined using Google Earth and images taken using a digital camera. One sampling site is  
255 completely under trees with dense canopy, where we cannot determine its exact coordinates  
256 using a GPS instrument or Google Earth imagery. In such a case, we used the location of the  
257 corresponding manhole (identified from the GIS data of the sewerage network) as the coordinates  
258 of the sampling site.

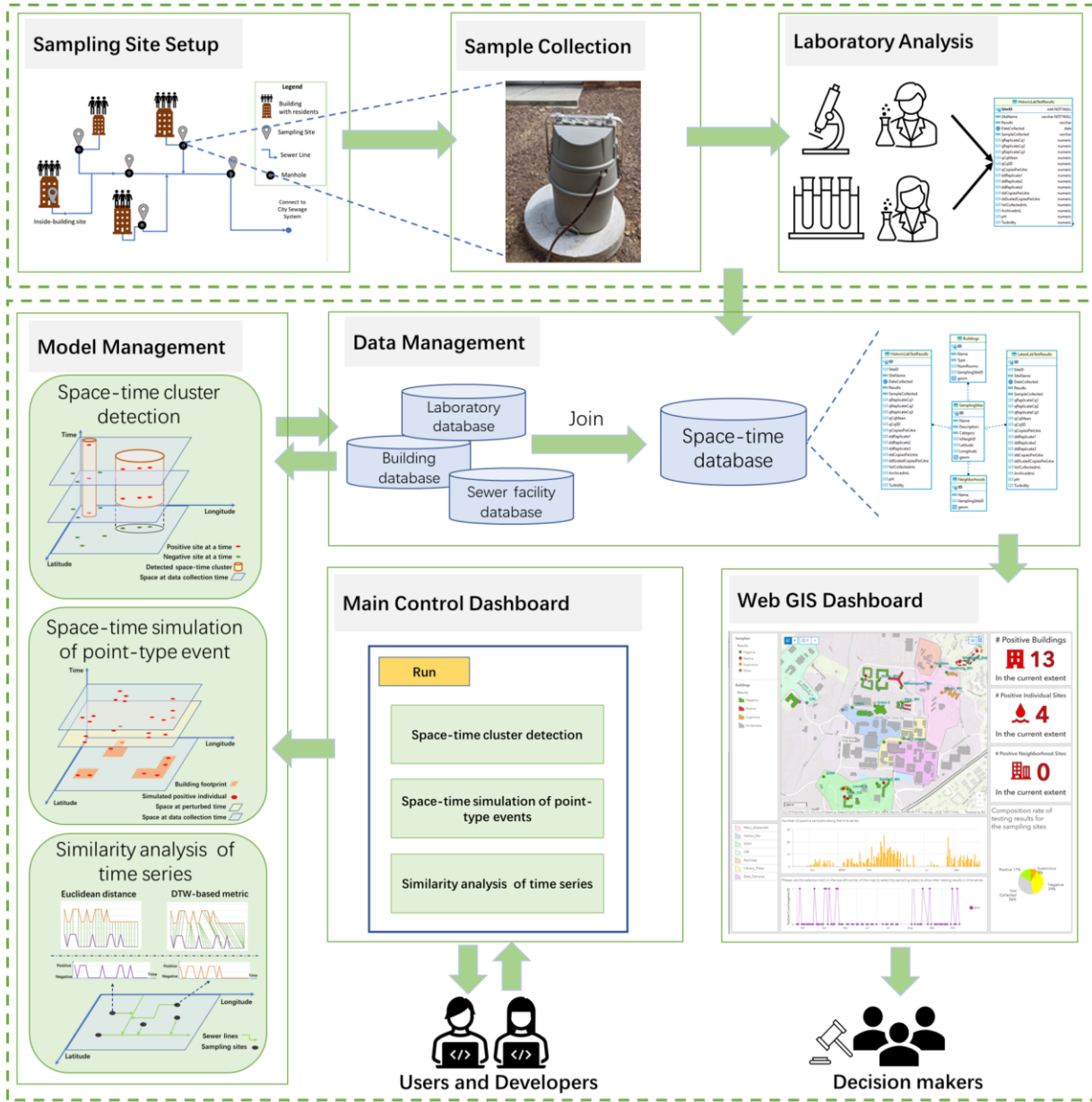


259  
260 **Fig. 2.** Illustration of sampling site setup for building-level wastewater surveillance.  
261

## 262 **3.2. Methods**

263 In this section, we present the framework of the web-based SDSS and its main components. Fig.  
264 3 illustrates the design of the web-based SDSS framework for wastewater surveillance in this  
265 study. This framework supports the data management, model management, and visualization of  
266 wastewater data that are spatiotemporally explicit. The integration of these functionality allows  
267 for the automated synchronization of wastewater testing results, on-demand spatiotemporal  
268 analysis of COVID-19 incidents from wastewater results, and automatic update of Web GIS  
269 dashboard that supports timely decision making in a spatially explicit manner.

270 Building-level wastewater surveillance typically includes three steps (see Gibas et al., 2021):  
271 collection of wastewater samples, sample concentration and RNA extraction, and detection of  
272 COVID-19 virus. Various sample-related data are generated from these steps. These data are  
273 characterized with space-time stamps and associated with different sampling sites, buildings, and  
274 sewersheds. Fundamentally, these data are space-time series that represent various information  
275 related to wastewater testing over space and time. Mathematically, our wastewater surveillance  
276 data (noted as  $W$ ) can be formulated as in Eq. 1:



277  
 278 **Fig. 3.** Framework of the web-based spatial decision support system for wastewater surveillance.  
 279

280 
$$W = \{ W(i,t) \mid W(i,t) = \{ id, w, v_1, v_2, \dots, v_p \} \}$$
 (1)

281 where:

282  $i$ : sampling site ID,  $i \in [1, 2, \dots, n]$ ;  $n$ : number of sampling sites;

283  $t$ : ID of time step;  $t \in [t_1, t_2, \dots, t_m]$ ;  $t_1$ : beginning date of wastewater sampling;  $t_m$ :  
 284 end date of sampling;  $m$ : number of sampling dates;

285  $id$ : ID of the sample at site  $i$  and time  $t$ .  
286  $w(i,t)$ : wastewater testing result for site  $i$  at time  $t$  ( $w(i,t)=\{0,1\}=\{\text{negative, positive}\}$ );  
287  $v_1(i,t), v_2(i,t), \dots, v_p(i,t)$ : all other variables associated with site  $i$  at time  $t$ ; These variables  
288 may change over time or not (e.g., testing results will change over time but the ID of  
289 associated building(s) will not).  
290  $p$ : number of other variables for a sampling site;  
291 Among these variables, the wastewater testing result  $w(i,t)$  is a binary variable that indicates  
292 whether COVID-19 virus is detected (1: positive; 0: negative) for a sampling site on a specific  
293 date. In this study, qPCR detection results from three sample replicates are used to determine  
294 whether a sample is considered positive or not. When the virus concentration (mean Cq) values  
295 of all three sample replicates are lower (indicating higher viral load) than the empirically  
296 determined limit of detection threshold, the corresponding wastewater sample is considered  
297 positive. For the purposes of determining administrative response on campus, samples must have  
298 all three replicates producing signals to be considered “positive”. Any samples that have only  $\frac{2}{3}$   
299 replicates producing signals are considered “suspicious” and 1 or fewer replicates producing  
300 signals considered negative. This “suspicious” designation is only used for administrative  
301 decision purposes. For more detail, please refer to Gibas et al. (2021). In our study here, samples  
302 that have 2 or less replicates producing signals are treated as negative (i.e., suspicious and  
303 negative samples are merged into a single category: negative).

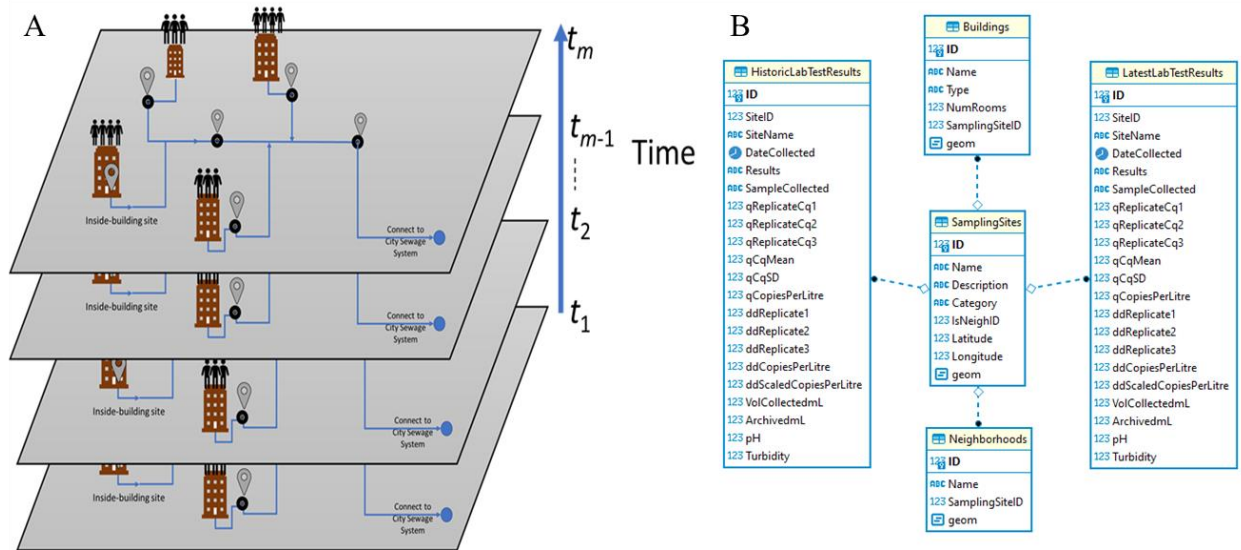
### 304 **3.2.1. Spatiotemporal data management and data synchronization**

305 We developed an object-based spatiotemporal data model (see Fig. 4A) to represent  
306 spatiotemporally explicit information related to building-level wastewater surveillance for  
307 COVID-19 monitoring. Spatiotemporal data models have been developed to represent dynamic  
308 geospatial phenomena (Chen et al., 2016; Pelekis et al., 2004; Peuquet & Duan, 1995). Based on



309 spatiotemporal data models, data structures and databases can be designed and implemented to  
310 handle data with spatiotemporal stamps. A series of spatiotemporal data models have been  
311 proposed in the literature, including snapshot-based, event-based, and object-based (Pelekis et  
312 al., 2004). Our spatiotemporal data model is object-based, in which a spatiotemporal object  
313 represents a geospatial entity in space and time. As the geometry of sampling sites and buildings  
314 does not change, our spatiotemporal data model only needs to take into account change in  
315 attributes (non-spatial information) associated with sampling sites or buildings. Thus, a  
316 wastewater sample collected at a site at a specific date is abstracted as a spatiotemporal object  
317 associated with a set of variables, including sampling site information (geometry: point),  
318 building information (geometry: footprint polygon), and lab testing results. Fig. 4B is the entity-  
319 relationship (ER) diagram that we used to build the geodatabase based on the spatiotemporal data  
320 model. Database tables were created to manage the spatiotemporal data associated with  
321 wastewater surveillance (including sampling sites, buildings, sewersheds, historic lab testing  
322 results, and latest lab testing results). Further, we used a set of database tables to maintain the  
323 relationships between sampling sites and buildings, as well as sampling sites and sewersheds.

324 We developed an automated synchronization module to upload wastewater testing results once  
325 they are available (including real-time and historic data). This automated data synchronization  
326 module is implemented within a web-based interface. This synchronization module takes sample  
327 testing results (in a delimited file; CSV format) as input and associates these testing results with  
328 corresponding buildings or sewersheds (through SQL style left-joins). Then, these testing results  
329 are updated to the spatiotemporal database.



330

331 **Fig. 4.** Illustration of spatiotemporal data model (A) and entity-relationship diagram (B) for  
 332 building-level wastewater surveillance.

333

### 334 3.2.2. Spatiotemporal analysis of wastewater testing results

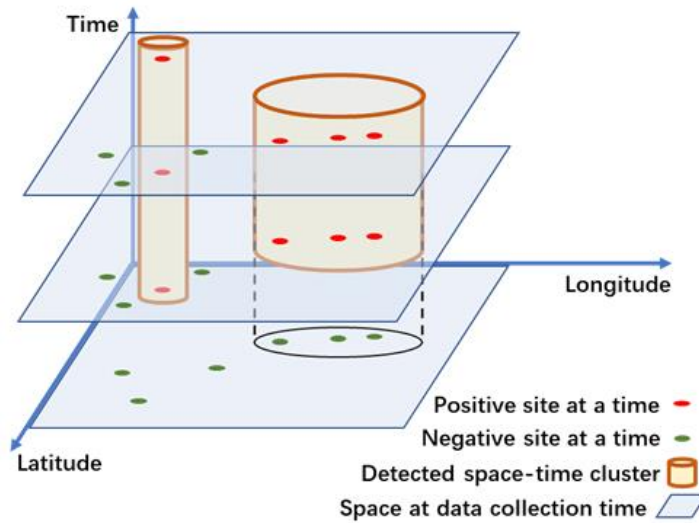
335 To address the research questions aforementioned in the Introduction section requires the use of  
 336 space-time analysis and modeling approaches. We chose to use space-time scan statistics, space-  
 337 time simulation of asymptomatic individuals, and similarity analysis of space-time series.

#### 338 3.2.2.1. Space-time scan for cluster detection

339 In this study, we utilized space-time scan statistics for the detection of space-time clusters of  
 340 positive wastewater samples reported from wastewater surveillance. We used Kulldorff's  
 341 retrospective space-time scan statistic (Kulldorff, 1999; Kulldorff et al., 1998), implemented in  
 342 SaTScan (version 9.6). A variety of studies have applied the space-time scan statistics approach  
 343 to detect clusters of covid cases during the COVID-19 pandemic (see, e.g., Desjardins et al.,  
 344 2020; Hohl et al., 2020; Kim & Castro, 2020; Masrur et al., 2020). However, the space-time

345 cluster detection for COVID-19 monitoring is often applied at large spatial or jurisdictional  
346 scales (e.g., state or county level for a country). To our knowledge, this is the first time that the  
347 space-time scan statistic is used to detect the presence of COVID19 in wastewater and at a small  
348 spatial scale (building level).

349 The space-time scan statistics uses a cylinder-based scanning window to detect the cluster of  
350 space-time objects (e.g., positive wastewater samples here; see Fig.5). The base of the cylinder  
351 defines the geographic region covered by the scanning window (the radius of the base is the  
352 spatial bandwidth) while the height represents the time duration of the scanning window (i.e.,  
353 temporal bandwidth). When applying space-time scan statistics, the center of the cylinder is  
354 placed at each spatial object (point-types; centroids can be used for polygon-type objects) and the  
355 spatiotemporal bandwidth is varied. Then, by using a likelihood ratio test, the number of  
356 observed events within and outside the cylinder is compared against their expected values based  
357 on Poisson or Bernoulli models (Kulldorff, 1997). Events within a cylinder scanning window  
358 with highest likelihood ratio (indication of elevated risk) are identified as a space-time cluster.  
359 Monte Carlo approach can be used to test the significance of the cluster(s). As the wastewater  
360 testing results are a binary variable (positive or negative) in this study, we used the Bernoulli  
361 model for the probability model used by the space-time scan statistics.



362

363 **Fig. 5.** Illustration of using cylindrical scanning windows for space-time scan statistics.

364

365 **3.2.2.2. Space-time simulation of asymptomatic individuals**

366 In this study, wastewater testing results from a sampling site are indicative of the situation of the  
 367 associated building(s)--whether there are presymptomatic individuals in the building. However,  
 368 the location of the individual(s) within the building is unknown (for privacy protection)—i.e.,  
 369 spatial uncertainty. Further, collected samples on a particular day may be reflective of a prior  
 370 contamination, keeping in mind that samples were collected every two days or more instead of  
 371 every day in our study—i.e., temporal uncertainty. Therefore, we used a space-time point pattern  
 372 simulation approach (see Diggle, 2013) to generate the locations of presymptomatic individuals  
 373 within the associated building (footprint in polygonal form) and the time that the individuals  
 374 begin to shed virus. In other words, this approach allows us to simulate space-time locations  
 375 (where and when) of the presymptomatic individuals, represented as space-time objects in this  
 376 study.

377 Fig. 6 illustrates the algorithm of the simulation of space-time point patterns of asymptomatic  
378 individuals within buildings. The space-time point pattern simulation begins with footprint  
379 polygons of all sampled buildings to determine the spatial location of an asymptomatic  
380 individual. A point is randomly generated within the bounding box of the footprint of each  
381 building. The point is retained if it is located within the building footprint polygon. Once the  
382 spatial location of the presymptomatic individual is determined, the date that the individual  
383 begins to shed virus is obtained by randomly perturbing the original sampling date up to  
384  $n\_perturb$  days before (e.g.,  $n\_perturb=3$  in this study). This procedure is applied to each  
385 building for a number of Monte Carlo repetitions (e.g., 1,000 repetitions used in this study).  
386 After the space-time location is determined, associated sampler site data and testing results are  
387 joined. The number of days for perturbation is based on the sampling frequency within a week.  
388 For example, 3 days could be used to cover the tri-weekly testing interval. Once simulated  
389 results are generated, space-time cluster analysis can be performed on these simulated  
390 spatiotemporal point patterns to examine the robustness of space-time clusters detected from  
391 observed data.

392

---

**Algorithm for simulation of spatiotemporal point patterns of asymptomatic individuals**

Parameters:

$n\_monte$ : number of Monte Carlo runs

$n\_perturb$ : number of days for temporal perturbation

Begin Algorithm

For each Monte Carlo run of  $n\_monte$  repetitions

For each sampling record (associated with a building and time)

Randomly generate a point within the building footprint for the sample site;

Randomly generate the time by perturbing sampling date up to  $n\_perturb$  days before;

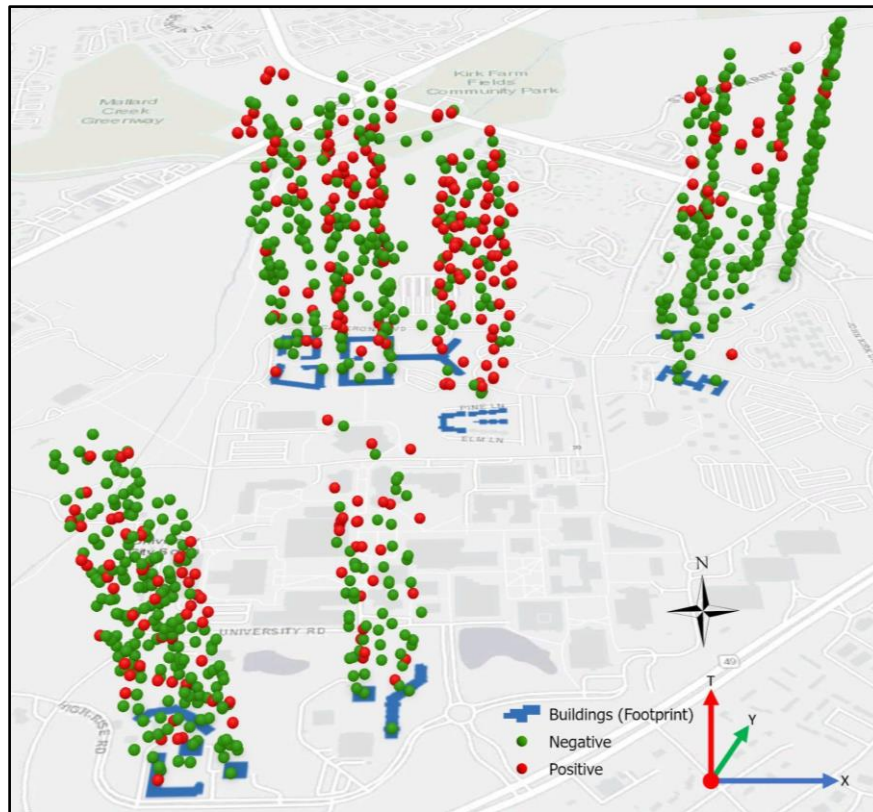
End for sampling record

End for Monte Carlo run

End Algorithm

---

393 **Fig. 6.** Algorithm of simulation of space-time locations of asymptomatic individuals.



395

396

397

398

399

400

**Fig. 7.** Illustration of a simulated space-time point pattern of asymptomatic individuals (simulated period: January 4<sup>th</sup>, 2021 to May 18<sup>th</sup>, 2021; number of samples: 926; number of positive samples: 264; number of days for perturbation: 3).

401

### 3.2.2.3. Similarity analysis of space-time series

402

To investigate whether any sampling sites show similar responses over time in terms of

403

wastewater testing results, we introduced similarity analysis of time series. We used two

404

similarity metrics, Euclidean distance-based and Dynamic Time Warping (DTW)-based, in this

405

study. Euclidean distance-based metric is a dissimilarity index that evaluates the distance of two

406

time series in the temporal dimension (see Choi et al., 2010). The DTW-based metric allows for

407

comparing time series in terms of shape (see Berndt & Clifford, 1994). DTW is a method that

408

computes the optimal matching between time series (or any sequence patterns) by minimization

408 of distances (Aghabozorgi et al., 2015; Berndt & Clifford, 1994). Given sampling site  $i$  and  $j$ ,  
 409 Euclidean distance-based metric (noted as  $D_{ij}$ ) between time series of their wastewater testing  
 410 results can be calculated by Eq. (2). The DTW-based measure (noted as  $DTW_{ij}$ ) is represented  
 411 using the shortest cumulative distance between the beginning and end time steps of wastewater  
 412 testing results at site  $i$  and  $j$  once matching between the two time series is optimized (see Eq. 3).

$$413 \quad D_{ij} = (\sum_{k=1}^m (w(i, t_k) - w(j, t_k))^2)^{1/2} \quad (2)$$

$$414 \quad DTW_{ij} = C_{ij}(m, m) = d_{ij}(m, m) + \min(C_{ij}(m-1, m-1), C_{ij}(m-1, m), C_{ij}(m, m-1)) \quad (3)$$

415 s.t.

$$416 \quad C_{ij}(0, 0) = 0;$$

$$417 \quad d_{ij}(k, l) = |w(i, t_k) - w(j, t_l)|$$

418

419 where  $D_{ij}$  and  $DTW_{ij}$  are the Euclidean distance metric and the dynamic time warping metric of  
 420 the time series between site  $i$  and  $j$ .  $w(i, t_k)$  is the binary testing result of sampling site  $i$  at time  $t_k$ ,  
 421 and  $w(j, t_l)$  the binary testing result site  $j$  at time  $t_l$  ( $k, l \in \{1, 2, \dots, m\}$ ;  $m$ : number of sampling  
 422 dates; defined in Eq. 1).  $C_{ij}(k, l)$  is the alignment cost between time step  $t_k$  of site  $i$  and time step  $t_l$   
 423 of site  $j$ .  $d_{ij}(k, l)$  is the distance between time step  $t_k$  of site  $i$  and time step  $t_l$  of site  $j$ .  $|\cdot|$  is the  
 424 absolute function that calculates the absolute distance between site  $i$  and  $j$ .  $\min(\cdot)$  is the function  
 425 to calculate the minimum of costs. The DTW-based measure is derived using a dynamic  
 426 programming approach (see Sakoe & Chiba, 1978). Each similarity measure is based on the  
 427 comparison of two time series, which leads to a  $n$  by  $n$  matrix of similarity for our wastewater  
 428 case ( $n$ : number of sampling sites; see Eq. 1). Once similarity measures are calculated,  
 429 hierarchical clustering can be applied to these similarity metrics to compare time series of  
 430 wastewater testing results of all sampling sites.

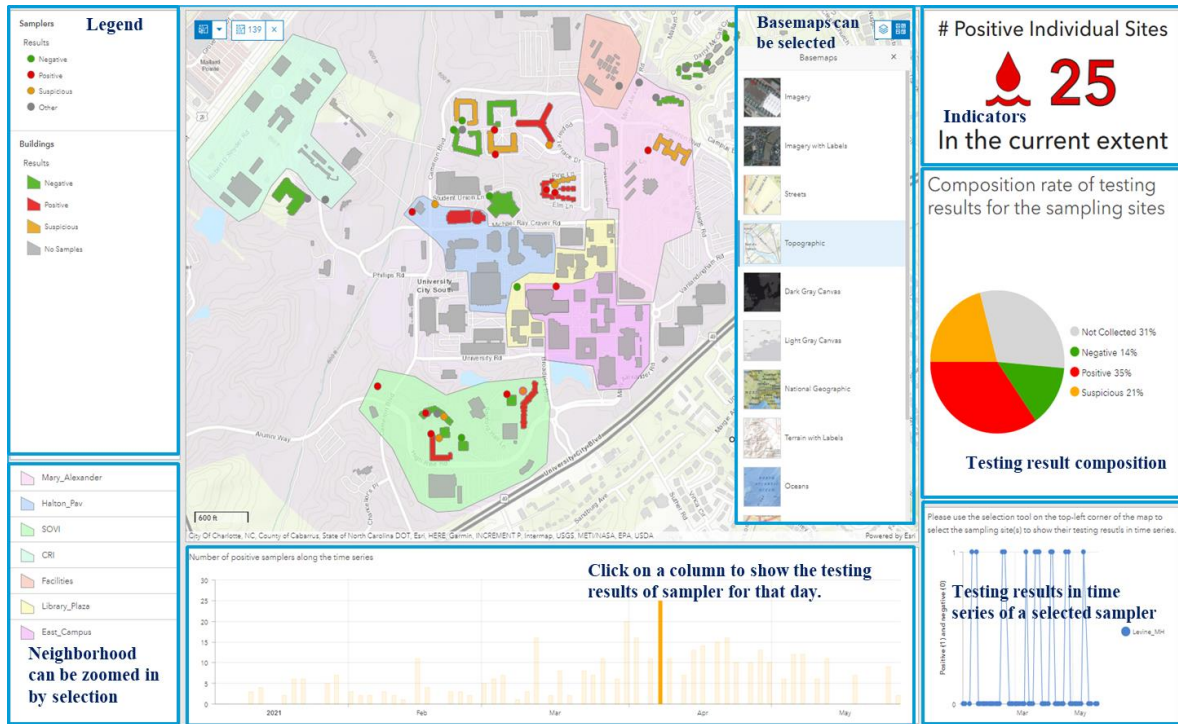
431

### 432 **3.2.3. Web-based mapping and geovisualization**

433 We used a Web GIS approach (Fu & Sun, 2011; see Peng & Tsou, 2003) for the visual  
434 presentation of wastewater data and related spatiotemporal analysis results. Based on the  
435 spatiotemporal data model, wastewater data are organized in a spatiotemporal database. We  
436 publish these spatially explicit data (sampling sites, sewage network, buildings) into geospatial  
437 web services that can be mashed up on a client-side web-based dashboard. When new  
438 wastewater testing results are available or the previous sample results are updated, the Web GIS  
439 module will automatically update these spatiotemporal data (via API) to the client-side web  
440 dashboard (including data, charts, and maps). Further, when new sampling sites are added or  
441 some existing sites are retired, the Web GIS module allows for updating spatial data and their  
442 geospatial web services (e.g., sampling sites in points, sewersheds in polygons).

443 We used Esri ArcGIS Online (<https://www.arcgis.com/>) for Web GIS-based dashboard and  
444 ArcGIS API for the automated update of wastewater data to the dashboard. Fig. 8 shows the  
445 snapshot of our Web GIS dashboard. The web mapping interface shows the locations of  
446 buildings, samplers, and sewersheds (aka, neighborhoods), and sewer networks (hidden for  
447 confidentiality consideration). Moreover, the color scheme of samplers and buildings indicate the  
448 sample testing results (shown in the map legend). Summary of wastewater testing results  
449 including number of positive buildings, sampling sites, sewershed sites, and their time series is  
450 displayed (for example, in charts). This provides visual and interactive analytics support that can  
451 inform decision makers for subsequent decision making on, for example, clinical testing or  
452 contract tracing.





453

454 **Fig. 8.** Snapshot of the Web GIS dashboard (sewer networks is hidden due to confidentiality  
 455 consideration).

456

457 **3.2.4. Implementation**

458 Our web-based SDSS is implemented within a web server. Jupyter Notebooks  
 459 (<https://jupyter.org/>) were used to implement the web-based main interface of the SDSS and  
 460 access to its individual modules. Table 2 shows the software or libraries used to implement each  
 461 individual module of the SDSS. We use ArcGIS API for Python to update wastewater testing  
 462 results to the Web GIS dashboard based on ArcGIS Online. Google OAuth was chosen as the  
 463 authentication mechanism of a web-based system for automated data synchronization.

464

465

466

467 **Table 2.** Software or libraries used by the web-based SDSS for wastewater surveillance.

Module name	Sub-module	Software/Library	URL
Module for geospatial database design and data synchronization	Web interface for data synchronization	ArcGIS API for Python (v1.9.1) Flask (v3.1)	<a href="https://developers.arcgis.com/python/">https://developers.arcgis.com/python/</a> <a href="https://flask.palletsprojects.com">https://flask.palletsprojects.com</a>
	Space-time cluster detection	SatScan	<a href="https://www.satscan.org/">https://www.satscan.org/</a>
Module for spatiotemporal analysis	Space-time simulation of point-type events	Python scripts	n/a
	Similarity measures of time series	TSdist v3.1 - Distance Measures for Time Series in R	<a href="https://cran.r-project.org/web/packages/TSdist/index.html">https://cran.r-project.org/web/packages/TSdist/index.html</a>
Module for web-based mapping and geovisualization	Web GIS dashboard	Esri ArcGIS Online	<a href="https://www.arcgis.com/index.html">https://www.arcgis.com/index.html</a>

468

469 **4. Results**

470 **4.1. Overall results**

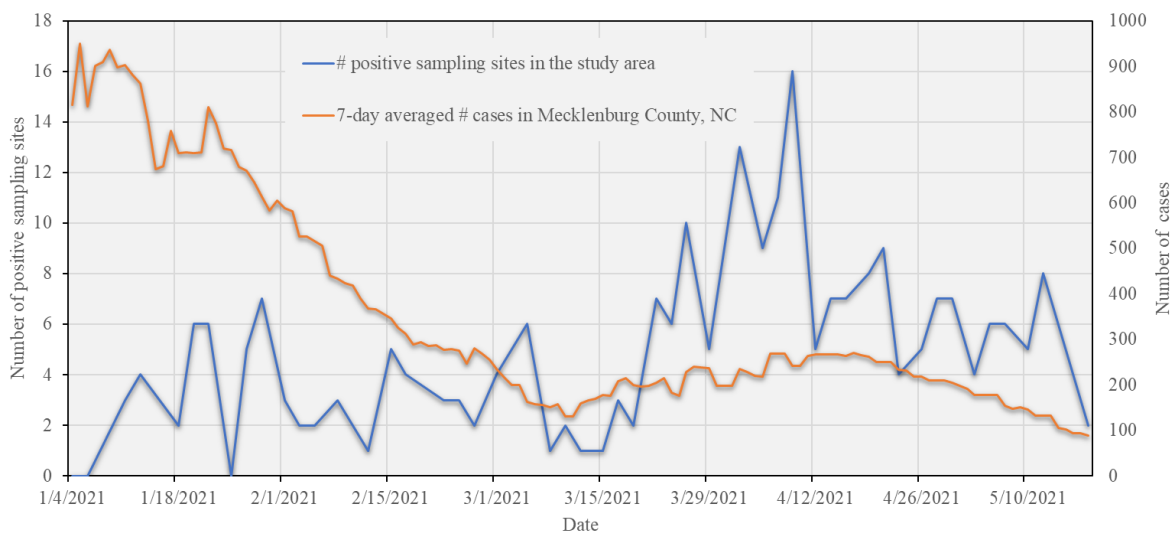
471 Our wastewater surveillance initiative has been collecting wastewater data since Fall 2020. We  
 472 have established 38 sampling sites since then. These sites provide strong support for monitoring  
 473 the COVID-19 situation via the wastewater surveillance approach. Wastewater testing results are  
 474 uploaded, synchronized, processed, analyzed, and visualized via the web-based SDSS. In this  
 475 study, we focus on using wastewater testing results from 23 residence hall sites from  
 476 01/04/2021 to 05/18/2021 (in total 135 days) as we have consistently used these sites to collect  
 477 samples during this period (results for neighborhoods sites and sampling sites of residence halls  
 478 that were established or removed during this period were excluded). Sewage samples were  
 479 collected three times a week on Monday, Wednesday, and Fridays for Spring 2021. This leads to

480 54 sample collections for each sampling site during the study period (18 weeks times 3  
481 collections per week). However, it is not always possible to collect a sample at every site every  
482 time due to variations in flow or unexpected physical obstruction of the autosampler probe. As a  
483 result, 926 samples were collected from these 23 sites for Spring 2021. Among them, there are  
484 662 negative (71.49%), and 264 positive (28.50%).

485 Fig. 9 depicts the number of positive sampling sites during the study period compared to the 7-  
486 day averaged number of cases in Mecklenburg County, NC (original data is retrieved from the  
487 U.S. Centers for Disease Control and Prevention, <https://ephtracking.cdc.gov/DataExplorer/>). As  
488 we could see, the number of positive sites fluctuates between 0 and 8 before March 24<sup>th</sup>, 2021.  
489 After that date, an increasing pattern in terms of the number of positive sampling sites can be  
490 observed and lasts for about 2 weeks. This number reaches its maximum (16) on April 9<sup>th</sup>, 2021.  
491 After April 9<sup>th</sup>, the number drops to under 10 and tends to show a decreasing pattern over time.

492 The spring semester of the University was postponed to start from January 20<sup>th</sup>, 2021 and Spring  
493 Break was changed to the week from February 8<sup>th</sup> to 13<sup>th</sup>, which was a decision made by the  
494 university due to the consideration of the pandemics (number of cases in Mecklenburg County is  
495 high in January and February; see Fig. 9). This explains the lower number of positive wastewater  
496 samples during the early stage of the semester. An increase in the number of cases in  
497 Mecklenburg County (corresponding to the local peak of the SARS-CoV-2 Alpha variant)  
498 appeared from mid March to mid April, 2021. Relaxation of local COVID-19 restrictions may  
499 also have contributed to this peak (see Executive Orders No. 195 and No. 204 by the North  
500 Carolina Governor on February 26<sup>th</sup> (NC government, 2021a) and March 26<sup>th</sup> (NC government,  
501 2021b)). This corresponds to (and may explain) a dramatic increase in the number of positive

502 samples on campus during that period. Decreasing trends appeared from mid to late April, 2021  
 503 in Mecklenburg County in terms of number of cases and on campus with respect to the number  
 504 of positive wastewater samples. This can be attributed to the availability of vaccines to more  
 505 people (increase in vaccination rate). Students started to receive vaccines beginning on March  
 506 31<sup>st</sup>, 2021, and vaccines were available to all adults in North Carolina by April 7<sup>th</sup> (Source:  
 507 <https://governor.nc.gov>). Two on-campus vaccine clinics (March 31<sup>st</sup>, 2021, and April 12<sup>th</sup>,  
 508 2021) hosted by the university facilitated vaccine uptake by students and faculty. All of these  
 509 vaccine-related events play an important role in contributing to the decreasing number of  
 510 positive samples in the final weeks of the semester.



511 **Fig. 9.** Number of positive sampling sites in the study area and 7-day averaged number of cases  
 512 in Mecklenburg County, NC over the study period.  
 513

514 **4.2. Results of space-time cluster analysis**

515 The use of space-time scan statistics needs to determine the upper limit of the spatiotemporal  
 516 cluster size bandwidth (spatial bandwidth and temporal bandwidth). For the upper limit of the  
 517 spatial bandwidth, we set the maximum spatial cluster parameter (corresponding to the

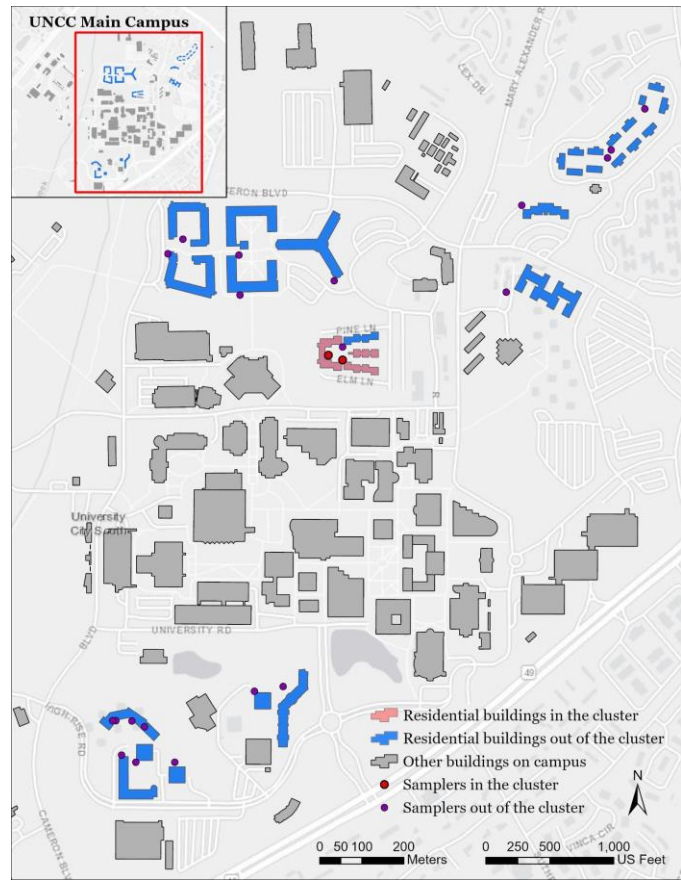
518 percentage of population at risk—i.e., number of collected samples for this study) as 50%. The  
 519 upper limit of the temporal bandwidth is set to 50% of the duration of the study period.

520 **4.2.1. Space-time cluster analysis results based on samples collected from sampling sites**

521 Fig. 10 and Table 3 depict the space-time scan results based on the collected samples for which  
 522 the locations of samplers were used as coordinates for space-time scan analysis. Fig. 10 shows  
 523 the map of detected space-time clusters. One significant cluster (p-value under 5%; based on 999  
 524 Monte Carlo runs) was detected that contains two sampling sites lasting from March 17<sup>th</sup>, 2021  
 525 to April 30<sup>th</sup>, 2021 (in total 44 days--about 7 weeks). These two sampling sites cover three  
 526 residence halls. Both the total number of collected samples (population for space-time scan) and  
 527 number of positive samples (cases) are 34, indicating all collected samples are positive in the  
 528 detected space-time cluster during these 7 weeks. The detection of this significant cluster is  
 529 because the three buildings have been used by the University for isolation and quarantine  
 530 purposes. The relative risk is 3.88 in the detected cluster, indicating the residence halls covered  
 531 by the sampling sites within the clusters are around 3-4 times higher than those out of the  
 532 clusters in terms of the ratio of number of positive samples over expected value.

533 Table 3. Information of the detected space-time cluster based on locations of sampling sites.

<b>Parameter</b>	<b>Value</b>	<b>Description</b>
Time span	3/17/2021 to 4/30/2021	Start date and end date of the cluster
Population	34	Number of collected samples
Number of cases	34	Number of positive samples
Expected cases	9.69	The number of samples within the cluster multiplied by the ratio of the total number of positive samples over the total number of samples for the entire study region.
Estimated risk	3.51	The ratio of the number of positive samples within the cluster over the number of expected cases within the cluster
Relative risk	3.88	The ratio of the estimated risk within the cluster over that outside of the cluster
p-value	5.2E-15 (p<=0.05)	p-value based on 1,000 Monte Carlo runs



534  
 535 **Fig. 10.** Map of the sampling sites in the detected cluster and corresponding residence halls  
 536 (sewer networks were hidden due to confidentiality consideration)

537  
 538 **4.2.2. Space-time cluster analysis results from simulated space-time point patterns**

539 The space-time scan results using locations of collected samples are based on sampling sites. In  
 540 our case study, these wastewater samples were contributed from individuals living in their  
 541 residence halls. Our sampling sites are, however, either outside or inside of residence halls, thus  
 542 posing an issue of locational uncertainty. To address this issue, we used the space-time  
 543 simulation of point-type events. We associate the binary (positive/negative) wastewater sampling  
 544 results from sampling sites back to the residence halls. For those sites that cover a single  
 545 building, once the wastewater testing result from any of these sites is positive, the residence hall  
 546 will exhibit a positive signal. For a sampling site that covers multiple buildings, all these covered

547 buildings will be positive if the testing results from the site are positive. The number of  
548 simulations for generating space-time point patterns was set to 1,000 in this study.

549 Fig. 11 shows the spatial pattern of residence halls within the detected clusters from 1,000  
550 simulated space-time point patterns (if a simulated presymptomatic individual within a building  
551 belongs to a cluster, then we consider the building is within the cluster). There are 8 residence  
552 halls that are within significant space-time clusters (at a 95% confidence level). We hide the  
553 names of the residence halls for confidentiality purposes. Table 4 summarizes the information of  
554 detected clusters based on the 1,000 simulated space-time point patterns. Relative risk within  
555 clusters is 2.774, indicating the estimated risk of residence halls within the cluster is 2-3 times  
556 higher than that outside the cluster.

557 Table 5 depicts start and end dates of each building within clusters, and Table 6 illustrates the  
558 number of weeks that the detected space-time clusters from 1,000 simulations last. Fig. 12 shows  
559 the histogram of the number of clusters in terms of the start date and end date of a building  
560 within detected clusters. It can be observed from Table 6 that detected clusters last from 1 week  
561 to 6 weeks, and 92.8% of the clusters last around 3-5 weeks. In general, the significant start date  
562 of clusters on each building at high risk concentrates on March 24<sup>th</sup>, 2021 (one exception is  
563 March 26<sup>th</sup> for building 7) and most of them end around April 23<sup>rd</sup> or 24<sup>th</sup> (April 20<sup>th</sup> for building  
564 7), lasting around 1 month. This suggests that the wastewater signals from these 8 buildings  
565 correspond to the second peak of the pandemic in Mecklenburg County (see Fig. 9). The three  
566 buildings used for isolation and quarantine purposes are included in these 8 buildings.



567  
 568 **Fig. 11.** Map of the residence halls in the detected clusters from simulated space-time point  
 569 patterns (number of simulations: 1,000)

570  
 571 Table 4. Summary of the clusters detected in 1,000 simulated datasets.

	Mean	Standard Deviation	Minimum	Maximum	Confidence Level for mean (95%)
Population	156.144	26.971	32	205	1.674
Number of cases	94.292	11.547	32	112	0.717
Expected cases	44.516	7.689	9.123	58.445	0.477
Estimated risk	2.145	0.167	1.901	3.508	0.010
Relative risk	2.774	0.129	2.544	3.904	0.008
P-value	1.08E-11	2.21E-11	6.99E-15	2.26E-10	1.37E-12

572  
 573



574 Table 5. Start and end dates of the buildings detected within clusters based on 1,000 simulations.

Building index	Start date (p<=0.05)	End date (p<=0.05)	Number of days at high risk
Building 1	March 23 <sup>rd</sup> , 2021	April 24 <sup>th</sup> , 2021	33
Building 2	March 23 <sup>rd</sup> , 2021	April 24 <sup>th</sup> , 2021	33
Building 3	March 23 <sup>rd</sup> , 2021	April 24 <sup>th</sup> , 2021	33
Building 4	March 23 <sup>rd</sup> , 2021	April 23 <sup>rd</sup> , 2021	32
Building 5	March 23 <sup>rd</sup> , 2021	April 23 <sup>rd</sup> , 2021	32
Building 6	March 23 <sup>rd</sup> , 2021	April 23 <sup>rd</sup> , 2021	32
Building 7	March 26 <sup>th</sup> , 2021	April 20 <sup>th</sup> , 2021	26
Building 8	March 23 <sup>rd</sup> , 2021	April 24 <sup>th</sup> , 2021	33

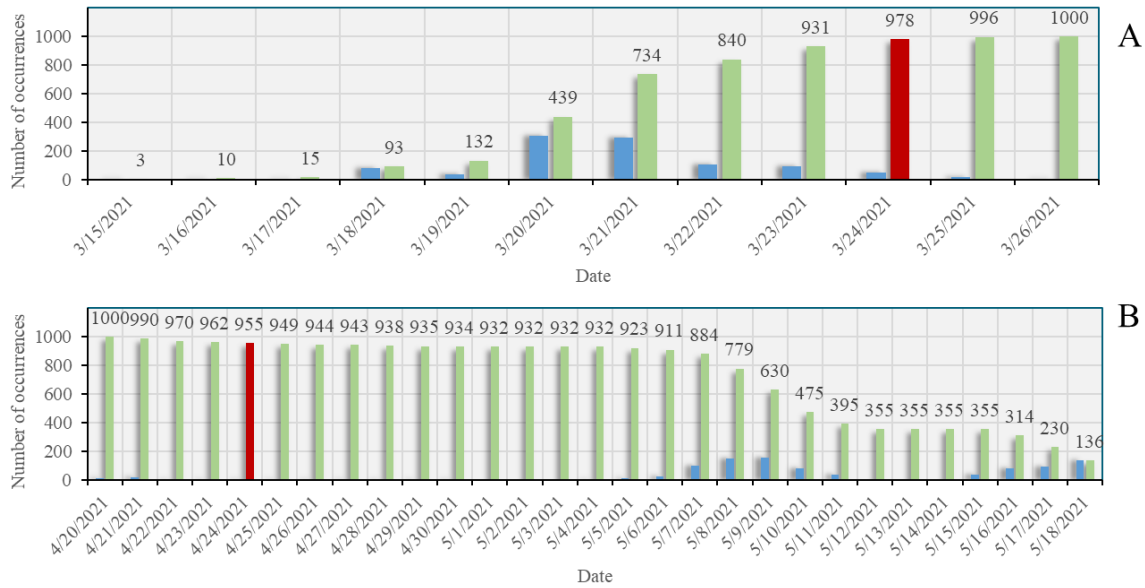
575

576 Table 6. Number of weeks covered by the space-time clusters detected from simulated patterns  
 577 (number of simulations: 1,000).

#Weeks	Frequency
1 week	53
2 weeks	18
3 weeks	254
4 weeks	384
5 weeks	290
6 weeks	1

578

579



580  
 581 **Fig. 12.** Histograms of the start (A) and end (B) dates that a building (Building 1) was identified  
 582 as within a cluster (blue) and the number of occurrences that a building was identified as within a  
 583 cluster over time (green) from simulations. Significant start and end dates (95% confidence  
 584 level) were colored in red. Number of simulations: 1,000.

585  
 586 The use of space-time scan for cluster analysis is computationally demanding because each  
 587 analysis would need additional 999 Monte Carlo runs for significance testing, and we need to  
 588 conduct this analysis on 1,000 simulated space-time point patterns of presymptomatic  
 589 individuals. To address this computational challenge, we deployed these analyses to a high  
 590 performance computing (HPC) cluster (computing node configuration: dual 24-Core Intel Xeon  
 591 Gold 6248R CPU with clock rate of 3.00 GHz and 384GB memory). Twenty computing nodes  
 592 (each with 24 cores--i.e., in total 480 CPUs) were used for acceleration. The parallel computing  
 593 time of the analysis of a single simulated point pattern on a computing node varies from 7.76 to  
 594 16.26 minutes with a mean of 8.42 minutes, while the mean sequential computing time for a  
 595 single analysis is 139.36 minutes. The total parallel computing time on 480 CPUs for 1,000  
 596 analyses is 7.08 hours, compared with the total sequential computing time (on a single CPU) of

597 2,322.72 hours (around 97 days). As a result, 327.91 times of acceleration was achieved for these  
598 analyses by using 480 CPUs.

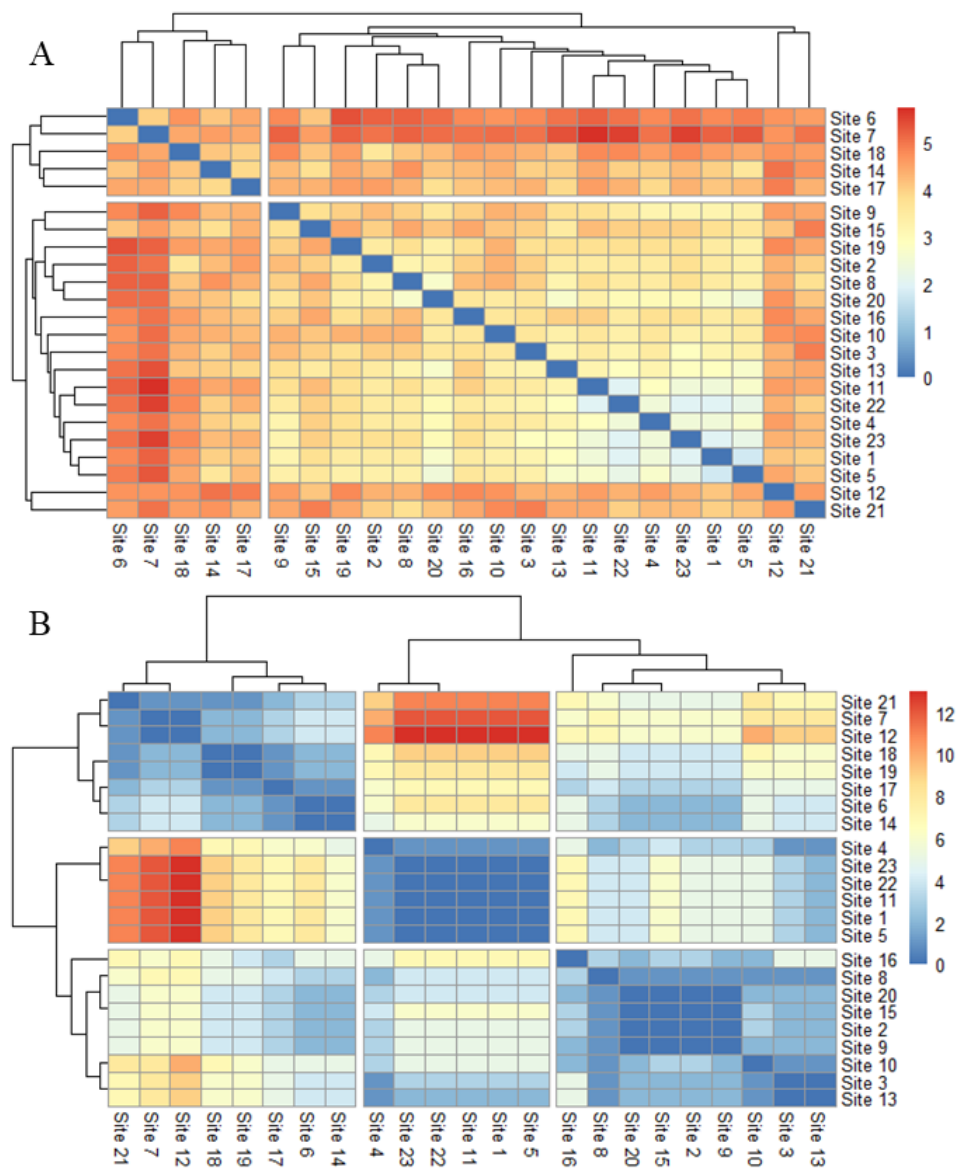
599

### 600 **4.3. Results of Similarity Analysis of Time Series**

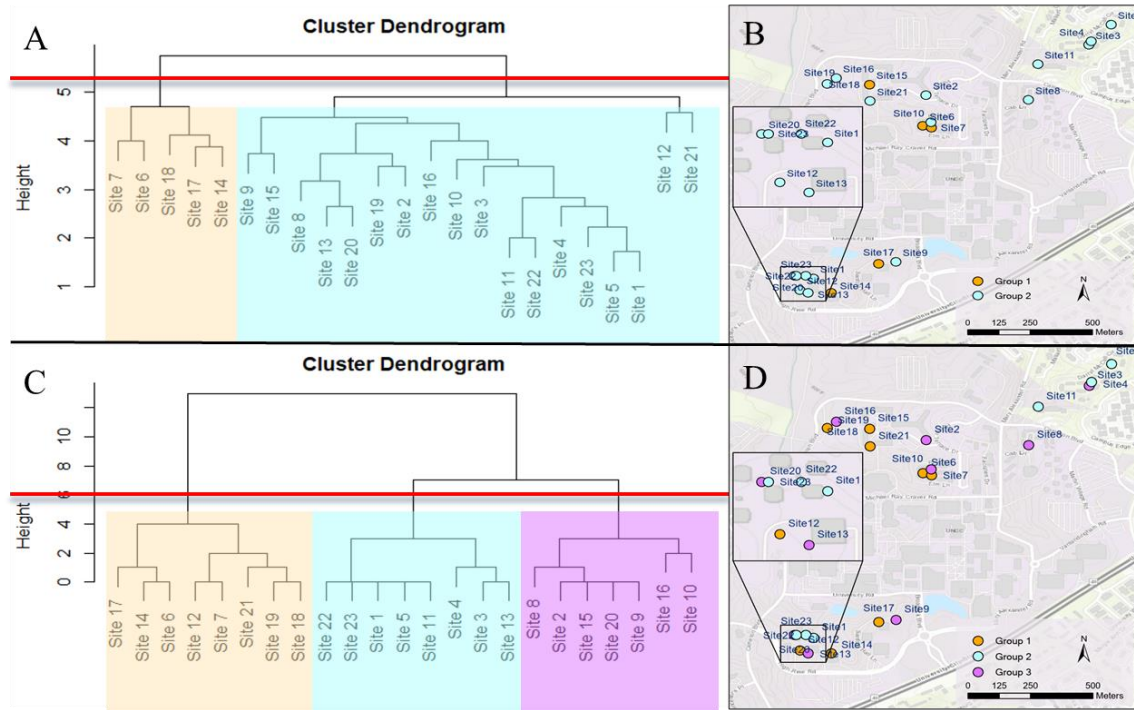
601 We conducted similarity analyses based on the time series of wastewater testing results from the  
602 23 sampling sites over the study period. Fig. 13 shows the results of similarity analysis with  
603 respect to metrics of Euclidean distance and DTW. Both Euclidean distance and DTW are  
604 dissimilarity metrics, meaning that the larger the value of the metrics, the more dissimilar the  
605 time series of two sites are. We then applied hierarchical clustering analysis to each of the two  
606 metrics. Elbow method (Thorndike, 1953) was used to determine the number of clusters based on  
607 these metrics. As a result, two clusters were identified with respect to the Euclidean distance  
608 metric and three clusters for the DTW metric.

609 Fig. 14 depicts the cluster dendrograms of the two similarity metrics as well as the spatial  
610 distribution of the identified clusters with respect to each of the similarity metrics. Fig. 15 shows  
611 the number of positive sites per week for each group identified by similarity metrics. The  
612 Euclidean distance-based metric clusters the sampling sites to two groups, whereas there are  
613 three main groups identified by the DTW metric. In terms of Euclidean distance-based metric  
614 (see Fig. 15A), group 1 covers five sampling sites, about 22% over 23 sampling sites in this  
615 study. The number of positive samples of group 1 fluctuates around 5 positive samples per  
616 collection day before and on March 15<sup>th</sup>, 2021. It rises to 10 - 15 positive samples per collection  
617 day from late March to mid April and then a decreasing trend appears until mid May. Group 2  
618 has 18 sampling sites, around three times higher than those in group 1. The number of positive

619 samples for each group in the study period tends to be close compared with the total number of  
 620 sampling sites in each group, indicating that buildings in group 1 are at higher risk of being  
 621 exposed under virus than those in group 2. We can also observe a rising pattern in the number of  
 622 positive samples for group 2 in mid March and a decreasing trend from late April to the end of  
 623 the study period.

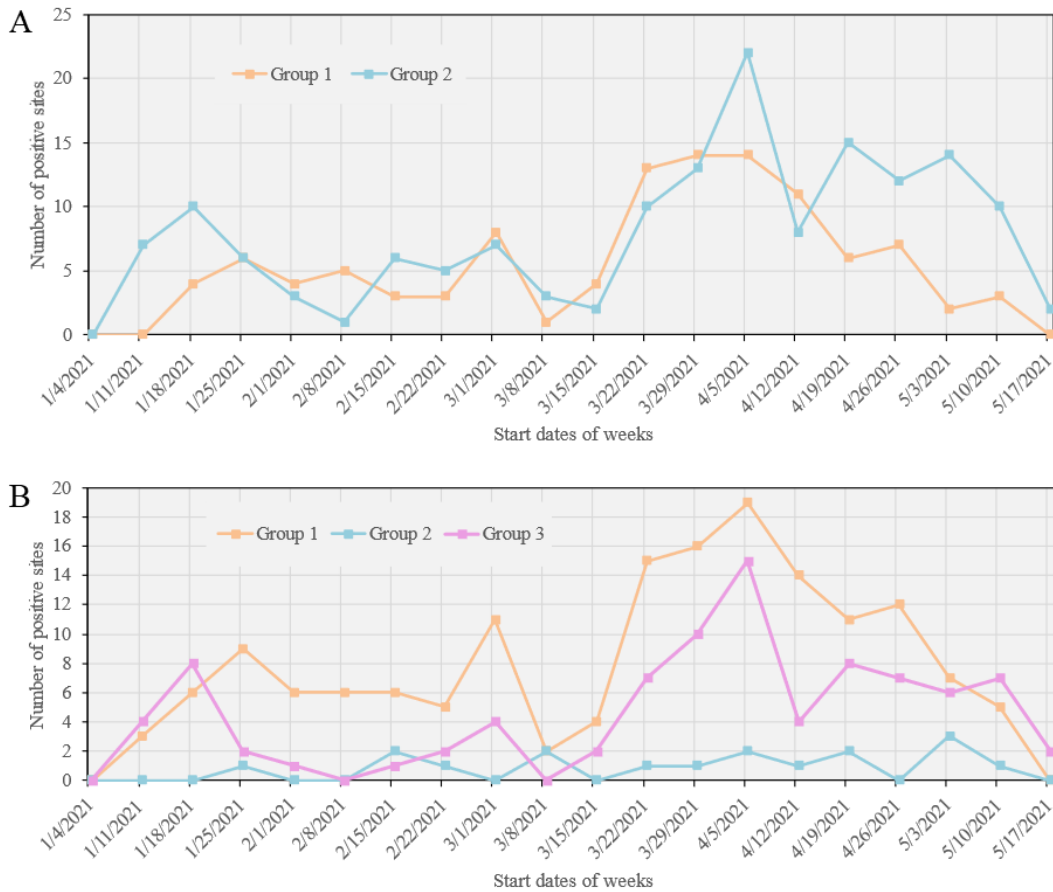


624  
 625  
 626 **Fig. 13.** Matrix of similarity metrics. (A: Euclidean distance; B: Dynamic Time Warping).



627  
 628  
 629  
 630  
 631  
 632

**Fig. 14.** Cluster dendrograms of similarity metrics and spatial patterns of clustered results. A and B are for Euclidean distance metric. C and D are for Dynamic Time Warping metric. The cut-off of the number of clusters (red line) was identified using the Elbow curves. Group 1, 2, and 3 were shaded in orange, blue, and purple.



633

634 **Fig. 15.** Number of positive sampling sites per week for each group identified by similarity  
 635 metric over time. A: for the Euclidean distance metric. B: for the Dynamic Time Warping metric.  
 636 The horizontal axis shows the start date of each week. The last week starting from May 17<sup>th</sup> only  
 637 has two-days data available.

638 With respect to the DTW metric (see Fig. 15B), three groups are identified, where the number of  
 639 sampling sites are 8, 6, and 9 for group 1, 2, and 3. It is observed that the weekly number of  
 640 positive samples in group 1 is higher than those of groups 2 and 3 in between January 25<sup>th</sup>, 2021  
 641 and May 3<sup>rd</sup>, 2021, covering most of the study period. The number of weekly positive samples in  
 642 group 2 is higher than that in group 3 especially in the beginning of the study period until  
 643 February 8<sup>th</sup>, 2021, and from March 15<sup>th</sup> to May 18<sup>th</sup>, 2021. Group 3 stays between 0 to 3  
 644 positive samples per week during this time span. Group 1 and 2 exhibit similar responses to the

645 spread of COVID-19 as we can observe three peaks in the time series: around January 20<sup>th</sup>,  
646 March 1<sup>st</sup>, and April 5<sup>th</sup>. Both group 1 and 2 strongly responded to the wave in Mecklenburg  
647 County, NC starting from mid March, 2021 (see Fig. 9); however, group 3 did not show a  
648 significant reaction to this wave, indicating residence halls in this group appear a relatively lower  
649 risk of being exposed to the virus than others during the study period.

650 Sites 6 and 7 identified in group 1 of both similarity metrics (see Fig. 14) are also detected within  
651 the cluster using space-time scan (see Fig. 10), indicating that buildings related to the two sites  
652 are more likely to be under exposure of the COVID-19 during the study period. Site 14, 17, and  
653 18 in group 1 for Euclidean distance are also included in the group 1 of DTW metric, indicating  
654 these sites also need to be paid attention. Further, group 1 of DTW metric suggests that site 12,  
655 19, and 21 are at relatively higher risk as well. Buildings in group 2 of the Euclidean distance  
656 metric appear less likely to be under exposure of the virus than those in group 1. It can be  
657 observed that buildings in group 2 and 3 detected by the DTW metric are included in group 2 of  
658 the Euclidean distance. Results in Fig. 15B also suggests that the two groups of DTW metric,  
659 especially group 2, appear to be characterized by a relatively low number of positive wastewater  
660 samples during the study period.

## 661 **5. Discussion**

662 Our web-based SDSS provides support for automating data operations, analysis and modeling,  
663 and visualization capabilities within an integrative environment. Wastewater surveillance is  
664 dependent on various data that may cut across different spatiotemporal scales. Our web-based  
665 SDSS allows for automated synchronization and mapping of these spatiotemporal data. This

666 provides timely support for the early detection of the COVID-19 virus in campus wastewater and  
667 thus greatly facilitates the monitoring and mitigation of the pandemic situation in the University.  
668 At the same time, the management of space-time wastewater data within this integrated  
669 environment can help monitor the status of samplers and their sampling sites. If any issues occur  
670 to the autosamplers that lead to the unavailability of samples over time, we could quickly  
671 identify and resolve the issues with support from this SDSS, thus ensuring the continual  
672 functioning of samplers.

673 Wastewater surveillance data are spatiotemporally explicit. Spatiotemporal analysis and  
674 modeling can be of great help in discovering interesting patterns in these spatiotemporal data,  
675 represented by the clusters of positive samples or residence halls detected using space-time scan  
676 approach and similarity analysis of space-time series in this study. The combination of the  
677 spatiotemporal analysis approaches has been suggested in the literature (see Xu & Beard, 2021).  
678 Space-time scan methods, represented by SatScan in this study, allows for detecting the co-  
679 occurrence of space-time events (positive samples in this study) within a specific time period  
680 (i.e., local- or regional-level analysis). Further, similarity analysis of space-time series offers a  
681 means of comparing space-time events over the entire study period--i.e., system-level  
682 comparison. Combining these spatiotemporal analysis methods enables us to discover patterns of  
683 interest from different levels (with respect to the study system of interest). On the one hand, this  
684 combined approach allows for identifying those residence halls where interactions with their  
685 residents are at a high risk during specific time periods. On the other hand, it gives us  
686 recommendations on the group of residence halls with a lower risk of virus even when it was  
687 peaking. This combined analysis approach provides substantial support for addressing



688 spatiotemporal questions (as in the Introduction section). It is also noted that the detection of  
689 these space-time clusters may be biased as samples may not be collected from every site each  
690 time, which will be investigated in future work. However, in general, these detected clusters  
691 from spatiotemporal analysis and modeling provide invaluable and critical support for the  
692 University on decisions or guidelines for the prevention of outbreak of the virus and control of  
693 virus transmission on campus.

694 The use of the space-time simulation of presymptomatic individuals was necessary because the  
695 relationship between sampling sites and their associated buildings is complicated (instead of one-  
696 to-one mapping) and because individuals in residence halls are sources that contribute to the  
697 wastewater testing results instead of samplers at sampling sites. The space-time scan results  
698 based on simulated individuals in residence halls are different than those based on sampling  
699 sites. The former approach detects more residence halls within the clusters of positive  
700 wastewater samples. The space-time simulation of the presymptomatic individuals provides an  
701 alternative approach for the possible locations of these individuals instead of relying on the  
702 sampling sites. While the detected clusters include more residence halls from space-time  
703 simulation, it is better than underestimating the number of residence halls that may exhibit strong  
704 positive signals of COVID-19 virus in wastewater. Of course, these clusters of positive  
705 wastewater samples are based on the space-time scan, which is a statistically based exploratory  
706 data analysis approach. The further interpretation of these clusters would require the expert  
707 knowledge from the collaboration of domain scientists (e.g., biogenetic professionals), better  
708 understanding of the wastewater surveillance system (e.g., sampling sites, residence halls,  
709 student interactions), and the incorporation of clinical testing and contact tracing data. In

710 particular, clinical testing data could be used to further improve the space-time simulation of  
711 presymptomatic individuals in terms of model calibration and validation. For example, in this  
712 study, wastewater samples that have 2 or less replicates producing signals are treated as negative.  
713 The use of clinical testing data could help us to fine tune the relationship between wastewater  
714 signals and infected individuals for more reliable spatiotemporal cluster analysis.

715 Web-based GIS is of essence in this web-based SDSS in terms of visual presentation of space-  
716 time data related to wastewater surveillance. Web-based GIS technologies and geospatial web  
717 services have been increasingly developed and available for the online management and mapping  
718 of spatially explicit data. However, the automatic update of data to Web GIS dashboards has  
719 been the bottleneck of Web GIS applications. Our web-based GIS and visualization module  
720 provides automation support that allows for the automatic update of wastewater sample data to  
721 the web GIS dashboard. Specifically, we aimed to reduce the time and number of steps that data  
722 are taken from the lab to the dashboard. This module will lead to the saving of tremendous time  
723 and cost as required by the update and dissemination of wastewater data that are continuously  
724 available over time.

## 725 **6. Conclusions**

726 The web-based SDSS framework presented in this study empowers the management, analytics  
727 and sharing of wastewater surveillance-related data at multiple spatiotemporal scales. The SDSS  
728 framework serves as a synergistic platform that integrates various types of data based on the  
729 spatiotemporal data model. Spatiotemporal analysis and modeling capabilities incorporated in  
730 this framework offer a means of unveiling interesting or unexpected patterns from the

731 wastewater data. These patterns may not be easily detected using visual inspection. These data-  
732 and model-related capabilities are managed and automated within the SDSS framework to ensure  
733 their reusability and the reproducibility of analytic results. This SDSS framework, built in with  
734 Web GIS dashboard functionality, will inform critical decision-making and guideline  
735 development for monitoring COVID-19 situations in the study region.

736 Future work of our study includes: 1) integration of 3D BIM-based building model into the web-  
737 based environment, 2) adding more spatial modeling capabilities (e.g., spatial simulation for  
738 scenario analysis and representation of individual behavior and social behavior using agent-  
739 based modeling; spatial optimization for optimal allocation of sampling sites), 3) use of  
740 continuous variable of virus concentration in wastewater samples instead of binary indicator for  
741 spatiotemporal analysis, and 4) extend the web-based SDSS framework to other or larger regions  
742 by, for example, linking to city sewage network and wastewater treatment plants at regional  
743 level.

744 **Acknowledgements**

745 The authors would like to thank Chancellor Sharon Gaber, Provost Joan Lorden, and Richard  
746 Tankersley, Vice Chancellor for Research and Economic Development and his team for strong  
747 institutional support of this wastewater surveillance project, Deborah Thomas, Chair of the  
748 Department of Geography and Earth Sciences for facilitating setting up geospatial computing  
749 needs for the project. The authors owe thanks to Facilities Management (Greg Cole) and OneIT  
750 (Alex Chapin, Elie Saliba) at the University of North Carolina at Charlotte for their support and  
751 help on sampling site setup and computing needs. High-performance computing resources used  
752 in this project were provided by University Research Computing at the University of North  
753 Carolina at Charlotte.

754

755 **Funding:**

756 The authors would like to thank financial support through CARES funding from NC General  
757 Assembly and funding from the University of North Carolina at Charlotte.

758 **References**

- 759 Aghabozorgi, S., Shirchorshidi, A. S., & Wah, T. Y. (2015). Time-series clustering—a decade  
760 review. *Information Systems*, 53, 16–38. <https://doi.org/10.1016/j.is.2015.04.007>
- 761 Ahmed, W., Tscharke, B., Bertsch, P. M., Bibby, K., Bivins, A., Choi, P., Clarke, L., Dwyer, J.,  
762 Edson, J., Nguyen, T. M. H., O’Brien, J. W., Simpson, S. L., Sherman, P., Thomas, K. V.,  
763 Verhagen, R., Zaugg, J., & Mueller, J. F. (2021). SARS-CoV-2 RNA monitoring in  
764 wastewater as a potential early warning system for COVID-19 transmission in the  
765 community: A temporal case study. *The Science of the Total Environment*, 761, 144216.  
766 <https://doi.org/10.1016/j.scitotenv.2020.144216>
- 767 Armstrong, M. P., Densham, P. J., & Rushton, G. (1986). Architecture for a microcomputer  
768 based spatial decision support system. *Second International Symposium on Spatial Data  
769 Handling, International Geographic Union*, 120–131.  
770 [https://iro.uiowa.edu/esploro/outputs/conferenceProceeding/Architecture-for-a-  
771 microcomputer-based-spatial/9983557551002771](https://iro.uiowa.edu/esploro/outputs/conferenceProceeding/Architecture-for-a-microcomputer-based-spatial/9983557551002771)
- 772 Barua, V. B., Juel, M. A. I., Blackwood, A. D., Clerkin, T., Ciesielski, M., Sorinolu, A. J.,  
773 Holcomb, D. A., Young, I., Kimble, G., Sypolt, S., Engel, L. S., Noble, R. T., & Munir, M.  
774 (2021). Tracking the temporal variation of COVID-19 surges through wastewater-based  
775 epidemiology during the peak of the pandemic: A six-month long study in Charlotte, North  
776 Carolina. *The Science of the Total Environment*, 152503.  
777 <https://doi.org/10.1016/j.scitotenv.2021.152503>
- 778 Becerik-Gerber, B., Jazizadeh, F., Li, N., & Calis, G. (2012). Application Areas and Data  
779 Requirements for BIM-Enabled Facilities Management. *Journal of Construction*

780        *Engineering and Management*, 138(3), 431–442. [https://doi.org/10.1061/\(ASCE\)CO.1943-](https://doi.org/10.1061/(ASCE)CO.1943-)  
781        7862.0000433

782        Berndt, D. J., & Clifford, J. (1994). Using dynamic time warping to find patterns in time series.  
783        *KDD Workshop*, 10, 359–370. <https://www.aaai.org/Library/Workshops/1994/ws94-03->  
784        031.php

785        Bowes, D. A., Driver, E. M., Kraberger, S., Fontenele, R. S., Holland, L. A., Wright, J.,  
786        Johnston, B., Savic, S., Newell, M. E., & Adhikari, S. (2021). Unrestricted Online Sharing  
787        of High-frequency, High-resolution Data on SARS-CoV-2 in Wastewater to Inform the  
788        COVID-19 Public Health Response in Greater Tempe, Arizona. *medRxiv*.  
789        <https://doi.org/10.1101/2021.07.29.21261338>

790        Chen, B. Y., Yuan, H., Li, Q., Shaw, S.-L., Lam, W. H. K., & Chen, X. (2016). Spatiotemporal  
791        data model for network time geographic analysis in the era of big data. *International*  
792        *Journal of Geographical Information Science*, 30(6), 1041–1071.  
793        <https://doi.org/10.1080/13658816.2015.1104317>

794        Choi, S. S., Cha, S. H., & Tappert, C. C. (2010). A survey of binary similarity and distance  
795        measures. *Journal of Systemics, Cybernetics and Informatics*, 8(1), 43–48.  
796        <http://citeseerx.ist.psu.edu/viewdoc/download?doi=10.1.1.352.6123&rep=rep1&type=pdf>

797        Ciesielski, M., Blackwood, D., Clerkin, T., Gonzalez, R., Thompson, H., Larson, A., & Noble,  
798        R. (2021). Assessing sensitivity and reproducibility of RT-ddPCR and RT-qPCR for the  
799        quantification of SARS-CoV-2 in wastewater. *Journal of Virological Methods*, 297,  
800        114230. <https://doi.org/10.1016/j.jviromet.2021.114230>

801        Crimi, A., Jones, T., & Sgalambro, A. (2019). Designing a Web Spatial Decision Support

802 System Based on Analytic Network Process to Locate a Freight Lorry Parking.  
803 *Sustainability: Science Practice and Policy*, 11(20), 5629.  
804 <https://doi.org/10.3390/su11205629>

805 Delmelle, E., Zhu, H., Tang, W., & Casas, I. (2014). A web-based geospatial toolkit for the  
806 monitoring of dengue fever. *Applied Geography*, 52, 144–152.  
807 <https://doi.org/10.1016/j.apgeog.2014.05.007>

808 Densham, P. J. (1991). Spatial decision support systems. In D. J. Maguire, M. F. Goodchild, &  
809 D. W. Rhind (Eds.), *Geographical Information Systems: Principles and Applications* (Vol.  
810 1, pp. 403–412). Hoboken, NJ: John Wiley & Sons.

811 Desjardins, M. R., Hohl, A., & Delmelle, E. (2020). Rapid surveillance of COVID-19 in the  
812 United States using a prospective space-time scan statistic: Detecting and evaluating  
813 emerging clusters. *Applied Geography*, 118, 102202.  
814 <https://doi.org/10.1016/j.apgeog.2020.102202>

815 Diggle, P. J. (2013). *Statistical Analysis of Spatial and Spatio-Temporal Point Patterns, Third*  
816 *Edition*. CRC Press.

817 Dong, E., Du, H., & Gardner, L. (2020). An interactive web-based dashboard to track COVID-19  
818 in real time. *The Lancet Infectious Diseases*, 20(5), 533–534.  
819 [https://doi.org/10.1016/S1473-3099\(20\)30120-1](https://doi.org/10.1016/S1473-3099(20)30120-1)

820 Fox, M. D., Bailey, D. C., Seamon, M. D., & Miranda, M. L. (2021). Response to a COVID-19  
821 outbreak on a University Campus—Indiana, August 2020. *Morbidity and Mortality Weekly*  
822 *Report*, 70(4), 118. <https://doi.org/10.15585/mmwr.mm7004a3>

823 Franch-Pardo, I., Napoletano, B. M., Rosete-Verges, F., & Billa, L. (2020). Spatial analysis and

824 GIS in the study of COVID-19. A review. *The Science of the Total Environment*, 739,  
825 140033. <https://doi.org/10.1016/j.scitotenv.2020.140033>

826 Fu, P., & Sun, J. (2011). *Web GIS: Principles and Applications*. Redlands, CA: Esri Press.

827 Ghosh, D. (2008). A loose coupling technique for integrating GIS and multi-criteria decision  
828 making. *Transactions in GIS*, 12(3), 365–375. <https://doi.org/10.1111/j.1467->  
829 9671.2008.01103.x

830 Gibas, C., Lambirth, K., Mittal, N., Juel, M. A. I., Barua, V. B., Roppolo Brazell, L., Hinton, K.,  
831 Lontai, J., Stark, N., Young, I., Quach, C., Russ, M., Kauer, J., Nicolosi, B., Chen, D.,  
832 Akella, S., Tang, W., Schlueter, J., & Munir, M. (2021). Implementing building-level  
833 SARS-CoV-2 wastewater surveillance on a university campus. *The Science of the Total*  
834 *Environment*, 782, 146749. <https://doi.org/10.1016/j.scitotenv.2021.146749>

835 Harris-Lovett, S., Nelson, K. L., Beamer, P., Bischel, H. N., Bivins, A., Bruder, A., Butler, C.,  
836 Camenisch, T. D., De Long, S. K., Karthikeyan, S., Larsen, D. A., Meierdiercks, K.,  
837 Mouser, P. J., Pagsuyoin, S., Prasek, S. M., Radniecki, T. S., Ram, J. L., Roper, D. K.,  
838 Safford, H., ... Korfmacher, K. S. (2021). Wastewater Surveillance for SARS-CoV-2 on  
839 College Campuses: Initial Efforts, Lessons Learned, and Research Needs. *International*  
840 *Journal of Environmental Research and Public Health*, 18(9), 4455.  
841 <https://doi.org/10.3390/ijerph18094455>

842 Hohl, A., Delmelle, E., Desjardins, M. R., & Lan, Y. (2020). Daily surveillance of COVID-19  
843 using the prospective space-time scan statistic in the United States. *Spatial and Spatio-*  
844 *Temporal Epidemiology*, 34, 100354. <https://doi.org/10.1016/j.sste.2020.100354>

845 Juel, M. A. I., Stark, N., Nicolosi, B., Lontai, J., Lambirth, K., Schlueter, J., Gibas, C., & Munir,



846 M. (2021). Performance evaluation of virus concentration methods for implementing  
847 SARS-CoV-2 wastewater based epidemiology emphasizing quick data turnaround. *The*  
848 *Science of the Total Environment*, 801, 149656.  
849 <https://doi.org/10.1016/j.scitotenv.2021.149656>

850 Karthikeyan, S., Nguyen, A., McDonald, D., Zong, Y., Ronquillo, N., Ren, J., Zou, J., Farmer,  
851 S., Humphrey, G., Henderson, D., Javidi, T., Messer, K., Anderson, C., Schooley, R.,  
852 Martin, N. K., & Knight, R. (2021). Rapid, Large-Scale Wastewater Surveillance and  
853 Automated Reporting System Enable Early Detection of Nearly 85% of COVID-19 Cases  
854 on a University Campus. *mSystems*. <https://doi.org/10.1128/mSystems.00793-21>

855 Keenan, P. B., & Jankowski, P. (2019). Spatial Decision Support Systems: Three decades on.  
856 *Decision Support Systems*, 116, 64–76. <https://doi.org/10.1016/j.dss.2018.10.010>

857 Kim, S., & Castro, M. C. (2020). Spatiotemporal pattern of COVID-19 and government response  
858 in South Korea (as of May 31, 2020). *International Journal of Infectious Diseases*, 98, 328–  
859 333. <https://doi.org/10.1016/j.ijid.2020.07.004>

860 Kırbıyık, U., Binder, A. M., Ghinai, I., & Zawitz, C. (2020). Network Characteristics and  
861 Visualization of COVID-19 Outbreak in a Large Detention Facility in the United States—  
862 Cook County, Illinois, 2020. *Morbidity and Mortality Weekly Report. Surveillance*  
863 *Summaries* , 69(44), 1625. <https://doi.org/10.15585/mmwr.mm6944a3>

864 Kulldorff, M. (1997). A spatial scan statistic. *Communications in Statistics: Theory and*  
865 *Methods*, 26(6), 1481–1496. <https://doi.org/10.1080/03610929708831995>

866 Kulldorff, M. (1999). Spatial scan statistics: Models, calculations, and applications. In *Scan*  
867 *Statistics and Applications* (pp. 303–322). Birkhäuser Boston. [49](https://doi.org/10.1007/978-</a></p></div><div data-bbox=)

868 1-4612-1578-3\_14

869 Kulldorff, M., Athas, W. F., Feurer, E. J., Miller, B. A., & Key, C. R. (1998). Evaluating cluster  
870 alarms: a space-time scan statistic and brain cancer in Los Alamos, New Mexico. *American*  
871 *Journal of Public Health*, 88(9), 1377–1380. <https://doi.org/10.2105/ajph.88.9.1377>

872 Lam-Hine, T., McCurdy, S. A., Santora, L., Duncan, L., Corbett-Detig, R., Kapusinszky, B., &  
873 Willis, M. (2021). Outbreak associated with SARS-CoV-2 B. 1.617. 2 (delta) variant in an  
874 elementary school—Marin County, California, May–June 2021. *Morbidity and Mortality*  
875 *Weekly Report. Surveillance Summaries*, 70(35), 1214.  
876 <https://doi.org/10.15585/mmwr.mm7035e2>

877 Lan, Y., Desjardins, M. R., Hohl, A., & Delmelle, E. (2021). Geovisualization of COVID-19:  
878 State of the art and opportunities. *Cartographica The International Journal for Geographic*  
879 *Information and Geovisualization*, 56(1), 2–13. <https://doi.org/10.3138/cart-2020-0027>

880 Lan, Y., Tang, W., Dye, S., & Delmelle, E. (2020). A web-based spatial decision support system  
881 for monitoring the risk of water contamination in private wells. *Annals of GIS*, 26(3), 293–  
882 309. <https://doi.org/10.1080/19475683.2020.1798508>

883 Lee, E. K., Pietz, F. H., Chen, C.-H., & Liu, Y. (2017). An interactive web-based decision  
884 support system for mass dispensing, emergency preparedness, and biosurveillance.  
885 *Proceedings of the 2017 International Conference on Digital Health*, 137–146.  
886 <https://doi.org/10.1145/3079452.3079473>

887 Liu, P., Ibaraki, M., VanTassell, J., Geith, K., Cavallo, M., Kann, R., Guo, L., & Moe, C. L.  
888 (2021). A sensitive, simple, and low-cost method for COVID-19 wastewater surveillance at  
889 an institutional level. *The Science of the Total Environment*, 151047.

890 <https://doi.org/10.1016/j.scitotenv.2021.151047>

891 Malczewski, J. (1999). *GIS and Multicriteria Decision Analysis*. Hoboken, NJ: John Wiley &  
892 Sons.

893 Marakas, G. M. (2003). *Decision support systems in the 21st century (Vol. 134)*. Upper Saddle  
894 River, NJ: Prentice Hall.

895 Masrur, A., Yu, M., Luo, W., & Dewan, A. (2020). Space-Time Patterns, Change, and  
896 Propagation of COVID-19 Risk Relative to the Intervention Scenarios in Bangladesh.  
897 *International Journal of Environmental Research and Public Health*, 17(16), 5911.  
898 <https://doi.org/10.3390/ijerph17165911>

899 Medema, G., Been, F., Heijnen, L., & Petterson, S. (2020). Implementation of environmental  
900 surveillance for SARS-CoV-2 virus to support public health decisions: Opportunities and  
901 challenges. *Current Opinion in Environmental Science & Health*, 17, 49–71.  
902 <https://doi.org/10.1016/j.coesh.2020.09.006>

903 Mwaura, D., & Kada, M. (2017). Developing a web-based spatial decision support system for  
904 geothermal exploration at the Olkaria geothermal field. *International Journal of Digital  
905 Earth*, 10(11), 1118–1145. <https://doi.org/10.1080/17538947.2017.1284909>

906 Naughton, C. C., Roman, F. A., Alvarado, A. G. F., Tariqi, A. Q., Deeming, M. A., Bibby, K.,  
907 Bivins, A., Rose, J. B., Medema, G., Ahmed, W., & Others. (2021). Show us the data:  
908 Global COVID-19 wastewater monitoring efforts, equity, and gaps. *medRxiv*.  
909 <https://doi.org/10.1101/2021.03.14.21253564>

910 NC government. (2021a, February 24). *Governor Cooper Announces Easing of COVID-19  
911 Restrictions as North Carolina Trends Stabilize*. <https://governor.nc.gov/news/press->

912 releases/2021/02/24/governor-cooper-announces-easing-covid-19-restrictions-north-  
913 carolina-trends-stabilize

914 NC government. (2021b, March 23). *Gov. Cooper Announces North Carolina Will Relax Some*  
915 *COVID-19 Restrictions*. [https://governor.nc.gov/news/press-releases/2021/03/23/gov-](https://governor.nc.gov/news/press-releases/2021/03/23/gov-cooper-announces-north-carolina-will-relax-some-covid-19-restrictions)  
916 [cooper-announces-north-carolina-will-relax-some-covid-19-restrictions](https://governor.nc.gov/news/press-releases/2021/03/23/gov-cooper-announces-north-carolina-will-relax-some-covid-19-restrictions)

917 NSF. (2007). *Cyberinfrastructure Vision for 21st Century Discovery*. National Science  
918 Foundation, Cyberinfrastructure Council. <https://www.nsf.gov/pubs/2007/nsf0728/>

919 Peccia, J., Zulli, A., Brackney, D. E., Grubaugh, N. D., Kaplan, E. H., Casanovas-Massana, A.,  
920 Ko, A. I., Malik, A. A., Wang, D., Wang, M., Warren, J. L., Weinberger, D. M., Arnold,  
921 W., & Omer, S. B. (2020). Measurement of SARS-CoV-2 RNA in wastewater tracks  
922 community infection dynamics. *Nature Biotechnology*, 38(10), 1164–1167.  
923 <https://doi.org/10.1038/s41587-020-0684-z>

924 Pelekis, N., Theodoulidis, B., Kopanakis, I., & Theodoridis, Y. (2004). Literature review of  
925 spatio-temporal database models. *Knowledge Engineering Review*, 19(3), 235–274.  
926 <https://doi.org/10.1017/s026988890400013x>

927 Peng, Z.-R., & Tsou, M.-H. (2003). *Internet GIS: Distributed Geographic Information Services*  
928 *for the Internet and Wireless Networks*. John Wiley & Sons.

929 Peuquet, D. J., & Duan, N. (1995). An event-based spatiotemporal data model (ESTDM) for  
930 temporal analysis of geographical data. *International Journal of Geographical Information*  
931 *Systems*, 9(1), 7–24. <https://doi.org/10.1080/02693799508902022>

932 Prado, T., Fumian, T. M., Miagostovich, M. P., & Gaspar, A. M. C. (2012). Monitoring the  
933 hepatitis A virus in urban wastewater from Rio de Janeiro, Brazil. *Transactions of the Royal*

934 *Society of Tropical Medicine and Hygiene*, 106(2), 104–109.  
935 <https://doi.org/10.1016/j.trstmh.2011.10.005>

936 Sakoe, H., & Chiba, S. (1978). Dynamic programming algorithm optimization for spoken word  
937 recognition. *IEEE Transactions on Acoustics, Speech, and Signal Processing*, 26(1), 43–49.  
938 <https://doi.org/10.1109/tassp.1978.1163055>

939 Sugumaran, R., & Degroote, J. (2010). *Spatial Decision Support Systems: Principles and*  
940 *Practices*. Boca Raton, FL: CRC Press.

941 Sweetapple, C., Melville-Shreeve, P., Chen, A. S., Grimsley, J. M., Bunce, J. T., Gaze, W.,  
942 Fielding, S., & Wade, M. J. (2022). Building knowledge of university campus population  
943 dynamics to enhance near-to-source sewage surveillance for SARS-CoV-2 detection. *The*  
944 *Science of the Total Environment*, 806, 150406.  
945 <https://doi.org/10.1016/j.scitotenv.2021.150406>

946 Tambini, G., Andrus, J. K., Marques, E., Boshell, J., Pallansch, M., de Quadros, C. A., & Kew,  
947 O. (1993). Direct detection of wild poliovirus circulation by stool surveys of healthy  
948 children and analysis of community wastewater. *The Journal of Infectious Diseases*, 168(6),  
949 1510–1514. <https://doi.org/10.1093/infdis/168.6.1510>

950 Tang, W., Feng, W., Jia, M., Shi, J., Zuo, H., Stringer, C. E., & Trettin, C. C. (2017). A cyber-  
951 enabled spatial decision support system to inventory Mangroves in Mozambique: coupling  
952 scientific workflows and cloud computing. *International Journal of Geographical*  
953 *Information Science*. <https://doi.org/10.1080/13658816.2016.1245419>

954 Tayyebi, A., Meehan, T. D., Dischler, J., Radloff, G., Ferris, M., & Gratton, C. (2016).  
955 SmartScape<sup>TM</sup>: A web-based decision support system<sup>TM</sup> for assessing the tradeoffs among

956 multiple ecosystem services under crop-change scenarios. *Computers and Electronics in*  
957 *Agriculture*, 121, 108–121. <https://doi.org/10.1016/j.compag.2015.12.003>

958 Thorndike, R. L. (1953). Who belongs in the family? *Psychometrika*, 18(4), 267–276.  
959 <https://doi.org/10.1007/BF02289263>

960 Xu, F., & Beard, K. (2021). A comparison of prospective space-time scan statistics and  
961 spatiotemporal event sequence based clustering for COVID-19 surveillance. *PloS One*,  
962 16(6), e0252990. <https://doi.org/10.1371/journal.pone.0252990>

963

964 **Appendix**

965 Appendix 1. Sources of the information about the University of North Carolina at Charlotte  
966 (retrieved year: 2021).

Sources	URLs
Faculty and Staff Resources	<a href="https://www.charlotte.edu/gateway/faculty-staff">https://www.charlotte.edu/gateway/faculty-staff</a>
Housing and Residence Life	<a href="https://housing.charlotte.edu/">https://housing.charlotte.edu/</a>
University Catalogs	<a href="https://catalog.uncc.edu/preview_program.php?catoid=30&amp;poid=8179">https://catalog.uncc.edu/preview_program.php?catoid=30&amp;poid=8179</a>
Housing and Residence Life	<a href="https://housing.charlotte.edu/housing-options/find-your-home">https://housing.charlotte.edu/housing-options/find-your-home</a>
Undergraduate Admissions	<a href="https://admissions.charlotte.edu/about-unc-charlotte/university-profile">https://admissions.charlotte.edu/about-unc-charlotte/university-profile</a>

967

968